METEOROLOGICAL OFFICE

Met O (APR) Turbulence and Diffusion Note No. 208

A Roughness Length for Temperature

by

Fiona Hewer

8th September 1993

Met O (APR)
(Atmospheric Processes Research)
Meteorological Office
London Road
Bracknell
Berks, RG12 2SZ

Note

A Roughness Length for Temperature

Fiona Hewer

8th September 1993

1 Introduction

This note is a summary of our investigation into a roughness length for temperature as a useful parameter for describing the boundary layer temperature profile. Its aim is to provide background and guidance for future work. It is the product of information gathered in several forums : a meeting at the Institute of Hydrology (IH); discussions at the European Geophysical Society (EGS) Assembly; sensitivity tests with the Single Column Unified Model (3.1); and a review of published work.

Much of the current research into a roughness length for temperature, z_{0t}, follows on from productive studies into a roughness length for momentum, z_{0m}. This parameter has proved a useful quantity in observational and modelling studies. The following Met. Office models use z_{0m} and are likely to benefit from a good understanding of z_{0t}.

- Unified Model
- Air Mass Transformation Model (Martin and Maryon (1992))
- Atmospheric Dispersion Modelling System (ADMS).

This note is organised into the following sections. Section 2 gives a theoretical background of z_{0t} for a homogeneous surface, first for a neutrally stratified surface layer and then for the more general context of an unstable or a stable surface layer. Alternative expressions to z_{0t} are described. Section 3 discusses some key problems with making observations. Parametrization and observations of z_{0t} over a flat, homogeneous surface are considered in section 4. These ideas are considered for heterogeneous terrain in section 5 and for hilly terrain in section 6. Section 7 reviews results from process modelling studies. The Discussion, section 8, describes the sensitivity of the Unified Model (UM) to z_{0t} and the factors that determine the appropriate value for z_{0t} in a General Circulation Model (GCM). Finally, the conclusions are given.

However, to begin, the basic theory of the logarithmic temperature profile is presented as a comparison to the logarithmic wind profile, anticipating that this will be more familiar to most readers.

2 Definitions of a roughness length for temperature over a flat, homogeneous surface.

2.1 The neutrally stratified atmospheric boundary layer.

Let us take the simplified case of mean horizontal flow in the x direction only, of speed U, in a neutrally stratified atmospheric boundary layer. In the surface layer, above homogeneous terrain, dimensional analysis gives an expression for the wind shear based on the assumption that the height above the surface is the only important length scale. So for a boundary layer of height, H, in the region where, $z_{0m} \ll z \ll H$ we may write,

$$\frac{\partial U}{\partial z} = \frac{u_*}{kz} \tag{1}$$

where k is von Kármán's constant, and u_* is the friction velocity defined in terms of the surface stress, τ, Nm^{-2} and the density ρ

$$\tau = \rho u_*^2 = -\rho\overline{u'w'} \tag{2}$$

As shown above, the surface stress can also be written in terms of the turbulent momentum flux or Reynolds flux, $\overline{u'w'}$ evaluated at the surface. This is a correlation of u and w deviations from mean values. w is the vertical component of motion.

Treating temperature as a passive scalar, we apply the same argument as for the shear (equation (1)) to the lapse rate. We will use temperature, T, where strictly potential temperature should be used but the two are very close in the surface layer (Brutsaert (1982)). Thus, in the region where, $z_{0m} \ll z \ll H$ we have,

$$\frac{\partial T}{\partial z} = \frac{-T_*}{kz} \tag{3}$$

where T_* is a reference temperature defined by the surface sensible heat flux, H_s, Wm^{-2}

$$H_s = \rho c_p u_* T_* = \rho c_p \overline{w'T'} \tag{4}$$

c_p is the specific heat capacity of air ($\approx 1000 Jkg^{-1}K^{-1}$). We see that the surface sensible heat flux can also be written in terms of the turbulent temperature flux evaluated at the surface, $Q \equiv \overline{w'T'}$. This is a correlation of w and T deviations. Here $Q > 0$ is chosen to mean a positive sensible heat flux, H_s, but some authors choose H_s to have the same sign as the lapse rate.

Now lets integrate the windshear equation (1), and lapse rate equation (3), side by side.

$$\int dU = \int \frac{u_*}{kz}dz \qquad \int dT = \int \frac{-T_*}{kz}dz$$

$$[U]_0^{U(z)} = \left[\frac{u_*}{k}\ln(z)\right]_{z_{0m}}^{z} \qquad [T]_{T_s}^{T(z)} = \left[\frac{-T_*}{k}\ln(z)\right]_{z_{0t}}^{z}$$

The limits of integration are chosen to relate a surface layer wind or temperature to some notion of a 'surface' value. For the momentum equation (1) we extrapolate the surface layer wind profile to a height beneath the surface layer, where $U = 0$ i.e. the no-slip condition applies: this height is the roughness length for momentum, z_{0m}. For the temperature equation (3), we extrapolate to a height where the temperature assumes a representative 'surface' value, T_s: this height is the roughness length for temperature, z_{0t}. So the roughness lengths for temperature and momentum creep in as constants of integration defined by,

$$U = 0 \quad \text{at} \quad z = z_{0m} \quad \text{and} \quad T = T_s \quad \text{at} \quad z = z_{0t} \tag{5}$$

Thus, evaluating the integrals we have,

$$U(z) = \frac{u_*}{k} \ln\left(\frac{z}{z_{0m}}\right) \qquad T_s(z_{0t}) - T(z) = \frac{T_*}{k} \ln\left(\frac{z}{z_{0t}}\right) \tag{6}$$

(7)

for $z_{0m} \ll z \ll H$ and $z_{0t} \ll z \ll H$, respectively.

There are four important things to notice about the log temperature profile equation which make it rather a different beast to the log wind profile. Firstly the left hand side is a profile difference so you can't get $T(z)$ from knowledge of the right hand side alone. Also, the surface layer temperature profile may increase or decrease with height, whereas wind speed will always increase. Thirdly, T_s and z_{0t} define each other i.e. z_{0t} is the height at which the surface layer temperature profile extrapolates to T_s and T_s is the temperature at z_{0t}. Therefore, the method of measuring the surface temperature will determine the value of z_{0t}. Finally, it depends both on the heat flux and the surface stress. 'Roughness' has some physical meaning for wind. In the log wind profile it represents the retardation effect of a surface on the flow over it. There doesn't appear to be any similar notion for z_{0t}.

We could integrate between any two heights within the surface layer to give a formula for wind/temperature at one height within the surface layer given values at any other, if we also know the surface stress and turbulent heat flux.

In all the equations we have considered so far, z has its origin at the surface but this definition will not work with our log profile theory if the atmosphere feels the surface to be higher than ground level eg where the vegetation is packed closely together. Figure 1 is a schematic diagram of the wind profile above such a surface.

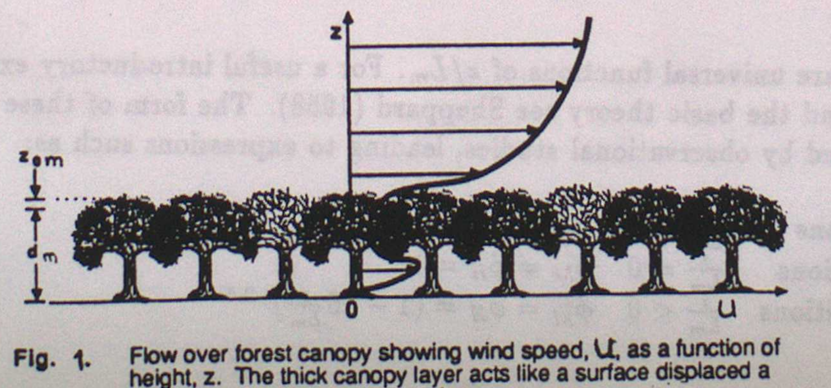

Fig. 1. Flow over forest canopy showing wind speed, U, as a function of height, z. The thick canopy layer acts like a surface displaced a distance, d, above the true surface.

z_{0m} is the roughness length for momentum of the branches and leaves to which the wind profile above will respond. It is the height above the *zero-plane displacement for momentum*, d_m metres, at which the surface-layer wind profile extrapolates to zero. A similar argument may be presented for the temperature profile above a densely vegetated surface, so that z_{0t} is defined relative to a *zero-plane displacement for temperature*, d_t metres. Therefore we must adapt our log profiles so they are rewritten as,

$$U(z) = \frac{u_*}{k} \ln\left(\frac{z - d_m}{z_{0m}}\right) \qquad T_s(z_{0t}) - T(z) = \frac{T_*}{k} \ln\left(\frac{z - d_t}{z_{0t}}\right) \tag{8}$$

(9)

Equation (5) becomes,

$$U = 0 \quad \text{at} \quad z = z_{0m} + d_m \quad \text{and} \quad T = T_s \quad \text{at} \quad z = z_{0t} + d_t \tag{10}$$

There does not seem to be any observational evidence to suggest what the relative sizes of d_m and d_t might be. However, if they are considered to be dynamical quantities related to eddy size and speed then we might expect that $d_m = d_t$ (Malhi, personal communication).

Figures 2 and 3 illustrate the relative importance of the quantities in the logarithmic temperature profile. Because it is a natural logarithm of z_{0t} that appears in the equation, factor of 10 changes to it make $\approx 2K$ changes to the temperature profile. In figures 2(a,b) temperature profiles have been diagnosed from selected typical values of $Q = \overline{w'T'}$, u_*, T_s for z_{0t} from 0.00001 to 0.1. The slope of the lines doesn't change because the heat flux and friction velocity are the same for each one.

Figures 3(a,b) shows the relative effect of increasing the surface sensible heat flux from 150 to 300 Wm^{-2} and decreasing z_{0t} by three orders of magnitude from 0.01 to 0.00001. At 10 metres, where the lines intersect, the effect is the same. Equivalently we could have halved the friction velocity.

2.2 Extension of the neutral profile theory.

The similarity theory developed by Monin and Obukhov extends the neutral theory above to other atmospheric states. They proposed that any dimensionless characteristic of the turbulence within the surface layer can depend only on, u_*, $\overline{w'T'}$, g/T_{ref} and z, i.e. upon z/L_m where $L_m = u_*{}^3 T_{ref}/kg\overline{w'T'}$ is the Obukhov stability length. Therefore equations (1) and (3) become,

$$\frac{\partial U}{\partial z} = \frac{u_*}{kz}\phi_M\left(\frac{z}{L_m}\right) \qquad \frac{\partial T}{\partial z} = \frac{-T_*}{kz}\phi_H\left(\frac{z}{L_m}\right) \tag{11}$$

(12)

where ϕ_H and ϕ_H are universal functions of z/L_m. For a useful introductory explanation of this extension and the basic theory see Sheppard (1958). The form of these functions has been determined by observational studies, leading to expressions such as:

stable conditions	$\frac{z}{L_m} > 0$	$\phi_M = \phi_H = 1 + 5\frac{z}{L_m}$
neutral conditions	$\frac{z}{L_m} = 0$	$\phi_M = \phi_H = 1$
unstable conditions	$\frac{z}{L_m} < 0$	$\phi_M^2 = \phi_H = (1 - 16\frac{z}{L_m})^{-0.5}$

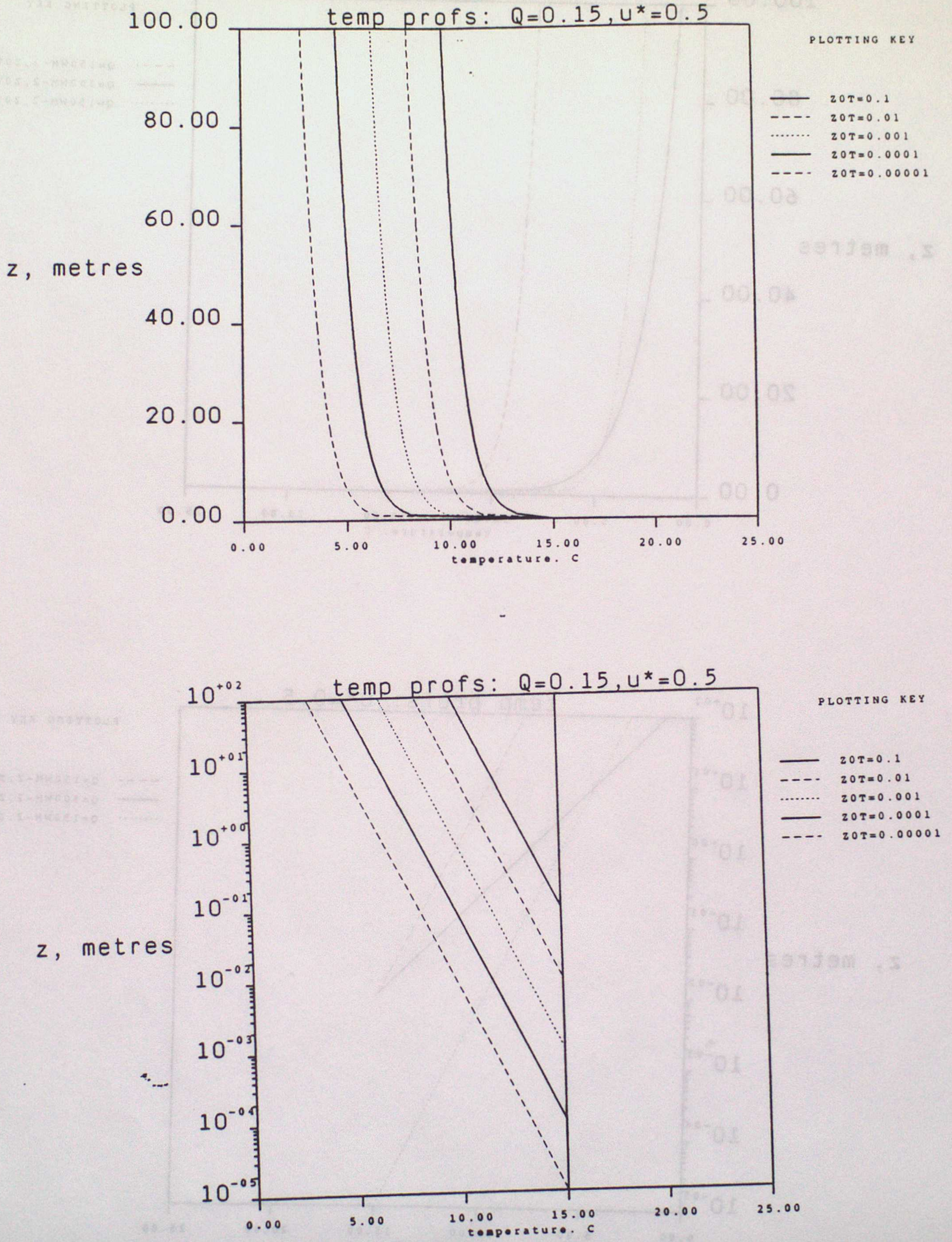

Figure 2. Temperature profiles from the neutral log profile equation with a range of roughness lengths for temperature.

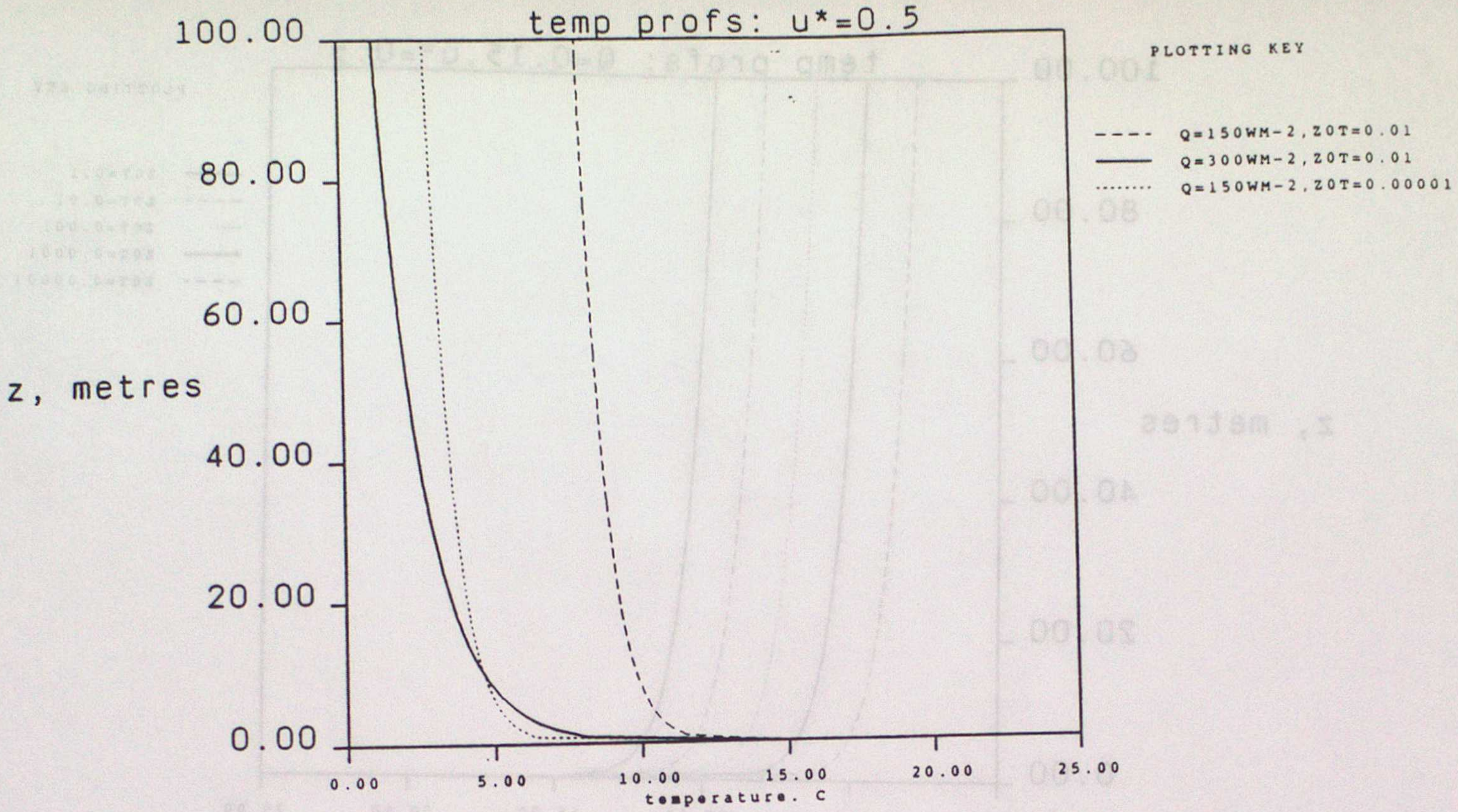

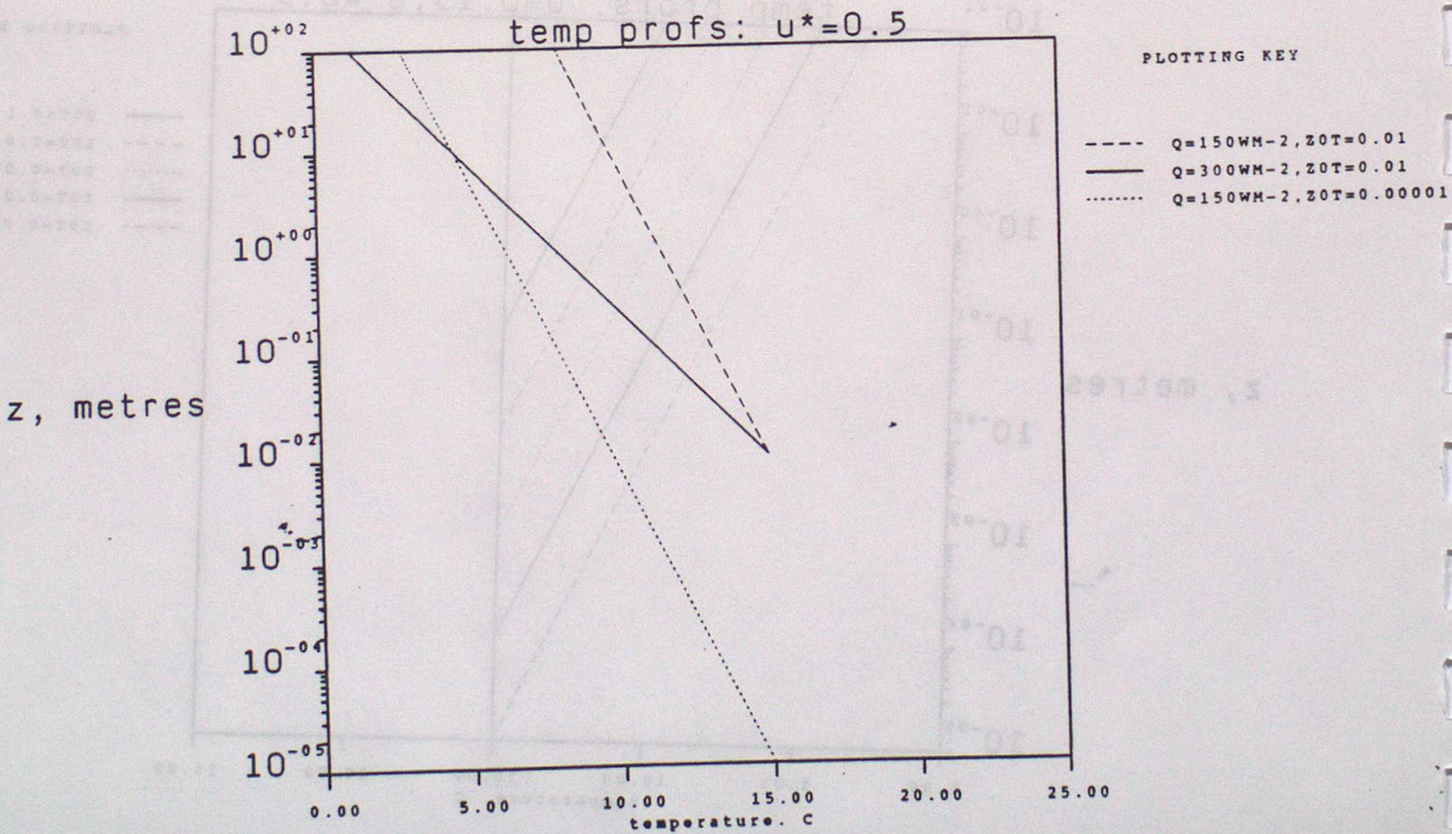

Figure 3. Temperature profiles from the neutral log profile equation comparing doubling $Q = \overline{w'T'}$ with reducing z_{0t}.

(eg see Businger (1988)). By assuming a lower limit of $z/L_m = z_{0t}/L_m \ll 1$ and also that $z/z_{0t} \gg 1$, we may integrate to yield (eg Garratt (1992), Chapter 3),

$$T(z) - T_s(z_{0t}) = -\frac{T_*}{k}\left[\ln(\frac{z}{z_{0t}}) - \psi_H(\frac{z}{L_m})\right] \tag{13}$$

where ψ_H is determined by integrating ϕ_H.

Now we have a mathematical description of the SURFACE LAYER temperature profile for unstable, neutral and stable boundary layers. They are defined in terms of z_{0t} and T_s which must be below the surface layer. It might be hoped that the height at which T_s is attained, ie z_{0t}, is the same as the extrapolated height of zero wind, z_{0m}, but this is not the case. Momentum transfer near the surface is dominated by the effect of a pressure gradient across roughness elements, with molecular diffusion playing a smaller part. However, heat is transferred by molecular diffusion alone (see eg Brutsaert 1975b). Therefore, we should not expect the roughness lengths for temperature and momentum to be the same.

2.3 Related quantities

Different research groups take different approaches to the problem of the surface layer temperature profile and consequently use z_{0t} in different guises.

Writing the momentum and heat fluxes in terms of the *drag coefficient*, C_D, and the *transfer coefficient*, C_H, we have,

$$\tau = \rho C_D U^2 \qquad H = \rho c_p C_H U(T_s - T) \tag{14}$$

(15)

where C_D and C_H are defined by,

$$C_D \equiv \frac{u_*^2}{U^2} \qquad C_H \equiv \frac{u_* T_*}{U(T - T_s)} \tag{16}$$

(17)

Substituting for u_* and T_* from the neutral log profiles gives,

$$C_{DN}(z) = \frac{k^2}{\left[\ln(\frac{z}{z_{0m}})\right]^2} \qquad C_{HN}(z) = \frac{k^2}{\ln\left(\frac{z}{z_{0m}}\right)\ln\left(\frac{z}{z_{0t}}\right)} \tag{18}$$

(19)

where N denotes neutral values. For the non-neutral case, from equation (13) we have,

$$C_H(z) = \frac{k^2}{(\ln(\frac{z}{z_{0m}}) - \psi_M(\frac{z}{L_m}))(\ln(\frac{z}{z_{0t}}) - \psi_H(\frac{z}{L_m}))} \tag{20}$$

Hydrologists and those with an interest in land-surface processes work in terms of *resistance* in units of sm^{-1}.

$$\tau = \frac{\rho U}{r_{am}} \qquad H = \frac{\rho c_p(T_s - T)}{r_{ah}} \tag{21}$$

(22)

Comparison with equations (14) and (15) reveals that,

$$r_{am} = \frac{1}{C_D U} \qquad r_{ah} = \frac{1}{C_H U} \tag{23}$$

(24)

Garratt and Hicks (1973) highlight the use of the *resistance ratio*, B also sometimes called the *sublayer Stanton number* (e.g. Chamberlain (1966)). Originally proposed by Owen and Thomson (1963), Chamberlain (1966) showed that it could be related to z_{0t} by

$$B^{-1} = \frac{1}{k} \ln \frac{z_{0m}}{z_{0t}} \tag{25}$$

where k is von Kármán's constant. It is a measure of the breakdown of the assumption that heat and momentum are transferred by the same mechanism. This quantity may be defined in terms of surface layer variables as,

$$B^{-1} = \frac{T - T_s}{T_*} - \frac{1}{k} \ln \left(\frac{z}{z_{0m}} \right) \tag{26}$$

which can be rearranged to relate the neutral drag and transfer coefficients,

$$C_{HN} = \frac{C_{DN}^{1/2}}{B^{-1} + C_{DN}^{-1/2}} \tag{27}$$

3 Problems with measuring z_{0t}.

A roughness length for temperature cannot be measured directly because it is a height reached by extrapolation down from the surface layer. To determine z_{0t} in neutral conditions we need measurements of the terms in equation (7) , i.e. 'surface' temperature, T_s, air temperature, T and the reference temperature, T_*. T_* may be calculated from the heat flux, and friction velocity u_*(see equation (4)).

The choice of method for measuring surface temperature is important because it will strongly influence our results. We have already seen from figure 2 that variation of $T - T_s$ by 2K changes z_{0t} by an order of magnitude. The surface temperature could be taken with a thermometer within the canopy, but the most sensible choice seems to be an airborne radiation thermometer. This gives us the equivalent black-body temperature of the canopy; it is applicable to numerical models and representative of a larger surface-area.

The heat flux can be calculated from profile measurements, the surface energy budget or eddy correlation techniques. The surface sensible heat flux is very sensitive to temperature profile measurements. This is demonstrated in Figure 4 after Sheppard (1958) which shows the sensitivity of heat flux calculations to wind and temperature gradients measured at two heights such that $z_2/z_1 = 2.0$.

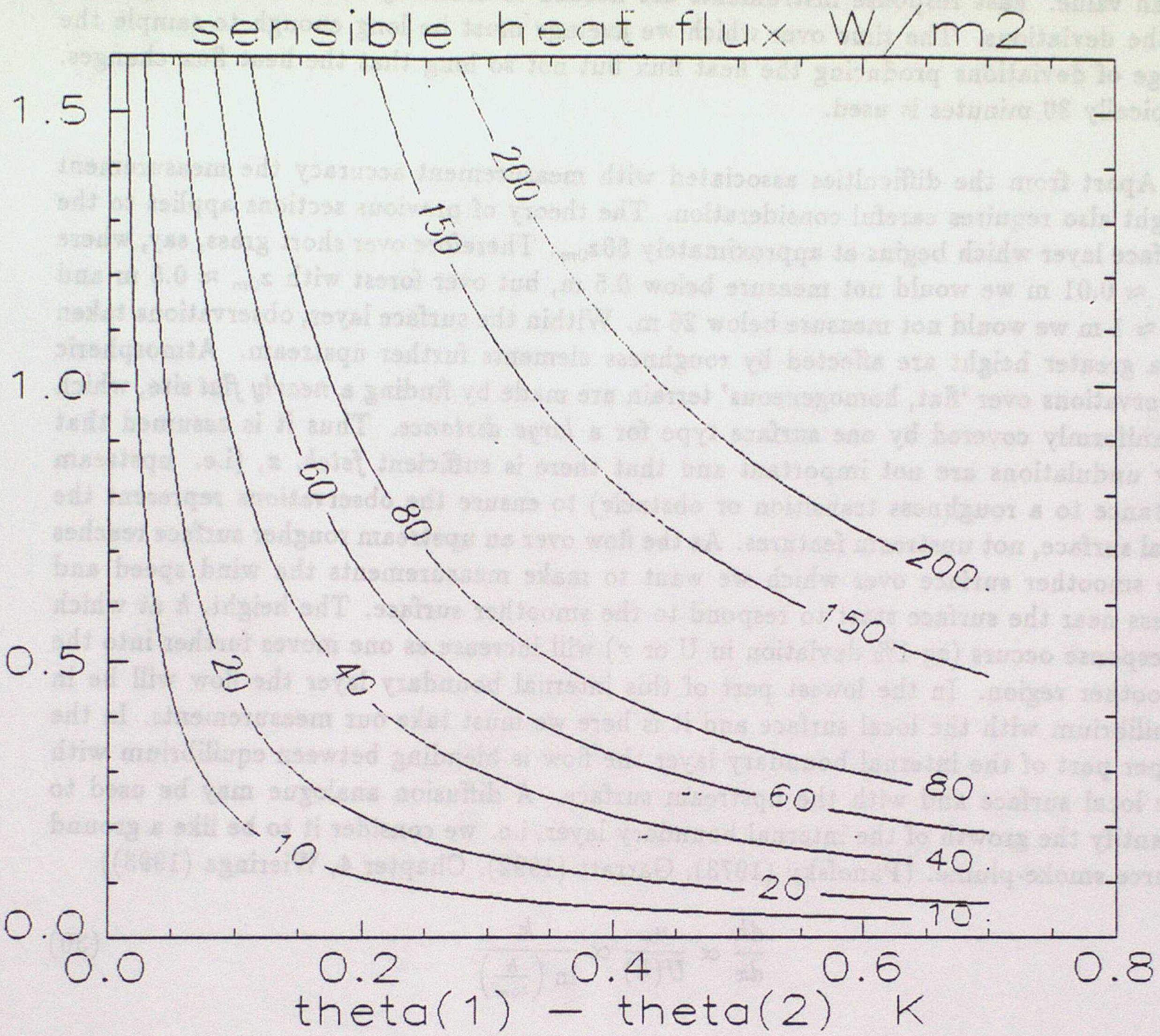

Figure 4. Contours of surface sensible heat flux from wind and temperature profiles after Sheppard (1958).

The equation for the heat flux

$$H_s = \rho c_p k^2 \frac{(U_2 - U_1)(T_1 - T_2)}{\left[\ln\left(\frac{z_2}{z_1}\right)\right]^2} \tag{27}$$

comes from integrating the logarithmic wind and temperature profiles between z_2 and z_1 and eliminating u_* and T_* from equation (4).

The heat flux can alternatively be determined from a surface energy balance

$$R - G = H + \lambda E \tag{28}$$

where $R\ Wm^{-2}$ is the surface net radiation, $G\ Wm^{-2}$ is the ground heat flux, $\lambda\ Jkg^{-1}$ is the latent heat of vaporization and $E\ kgm^{-2}s^{-1}$ is the evaporation. However, λE is a very difficult quantity to measure accurately.

The third possibility for calculating the heat flux is from eddy correlation measurements of $\overline{w'T'}$, and u_* from $\overline{u'w'}$. We must take a time average of deviations from the mean value. Fast response instruments are needed to correctly measure the magnitude of the deviations. The time over which we average must be long enough to sample the range of deviations producing the heat flux but not so long that the heat flux changes. Typically 30 minutes is used.

Apart from the difficulties associated with measurement accuracy the measurement height also requires careful consideration. The theory of previous sections applies to the surface layer which begins at approximately $50z_{0m}$. Therefore over short grass, say, where $z_{0m} \approx 0.01$ m we would not measure below 0.5 m, but over forest with $z_{0m} \approx 0.5$ m and $d_m \approx 1$ m we would not measure below 26 m. Within the surface layer, observations taken at a greater height are affected by roughness elements further upstream. Atmospheric observations over 'flat, homogeneous' terrain are made by finding a *nearly flat* site, which is uniformly covered by one surface type for a *large distance*. Thus it is assumed that any undulations are not important and that there is sufficient *fetch*, x, (i.e. upstream distance to a roughness transition or obstacle) to ensure the observations represent the local surface, not upstream features. As the flow over an upstream rougher surface reaches the smoother surface over which we want to make measurements the wind speed and stress near the surface start to respond to the smoother surface. The height, h at which a response occurs (eg 1% deviation in U or τ) will increase as one moves further into the smoother region. In the lowest part of this internal boundary layer the flow will be in equilibrium with the local surface and it is here we must take our measurements. In the upper part of the internal boundary layer the flow is blending between equilibrium with the local surface and with the upstream surface. A diffusion analogue may be used to quantify the growth of the internal boundary layer, i.e. we consider it to be like a ground source smoke-plume. (Panofsky (1973), Garratt (1992), Chapter 4, Wieringa (1993))

$$\frac{dh}{dx} \propto \frac{u_*}{U(h)} \propto \frac{k}{\ln\left(\frac{h}{z_{0m}}\right)} \tag{30}$$

Integration yields,

$$\frac{h}{z_{0m}^{smooth}}\left[\ln\left(\frac{h}{z_{0m}^{smooth}}\right) - 1\right] + 1 = \frac{Ax}{z_{0m}^{smooth}} \tag{31}$$

where $A \approx 1$. Model studies have shown that the flow is in local equilibrium with the surface at up to one tenth of the internal boundary layer height h. Thus over short grass, if we take $z_{0m}^{smooth} = 0.01$ m then the fetch required to take measurements at 2m is 260m. These ideas are based on momentum transport ideas, but give a simple estimate of the fetch requirements for turbulent flux measurements in general. Wood and Mason (1991) found that the height at which the flow is in equilibrium with the local surface is lower for temperature parameters, and so the fetch required is greater.

Claussen (1987) has also found that a *downstream* distance from a measurement site to a roughness transition of $\approx$300 z_{0m} is required to avoid modification of observations by the downstream surface.

For observations over heterogeneous terrain there is the further problem of determining which area of the upstream surface measurements at a particular height will represent. Then sub-areas must be identified and have a roughness length for temperature ascribed to them if we wish to test the averaging ideas discussed in section 5.2. Schmid and Oke (1990) have devised a *Source Area Model* to calculate the particular region of the upstream surface that contributes to turbulent fluxes at a point and height. Their model is based on a plume diffusion model, and applies only to unstable conditions. It requires as input: the measurement height, the roughness length for momentum, the Obukhov stability length (see section 2), the friction velocity and the standard deviation of cross-wind fluctuations. The output is a family of elliptical surface areas and source weight distributions each representing a proportion of the measurement explained by that area. For example, there is a probability of 0.5 that the measurement is influenced by the surface within the 0.5 source area isopleth. Figure 5 shows 0.3 (dashed lines) and 0.5 (solid lines) source area isopleths over Cabauw for measurement heights of 3.5m (smaller outlines) and 22.5m (larger outlines) calculated by Schmid and Oke using data from year-days 140, 161 and 174 of Beljaars (1983). The filled dots indicate the maximum source location. The 3.5m measurements have maximum sources between 27 and 36m from the tower, with the furthest part of the 0.5 isopleth $\simeq 200m$ away. The 22.5m measurements have their maximum sources between 160 and 350m away and the 0.5 isopleth extends to $\simeq$1500m.

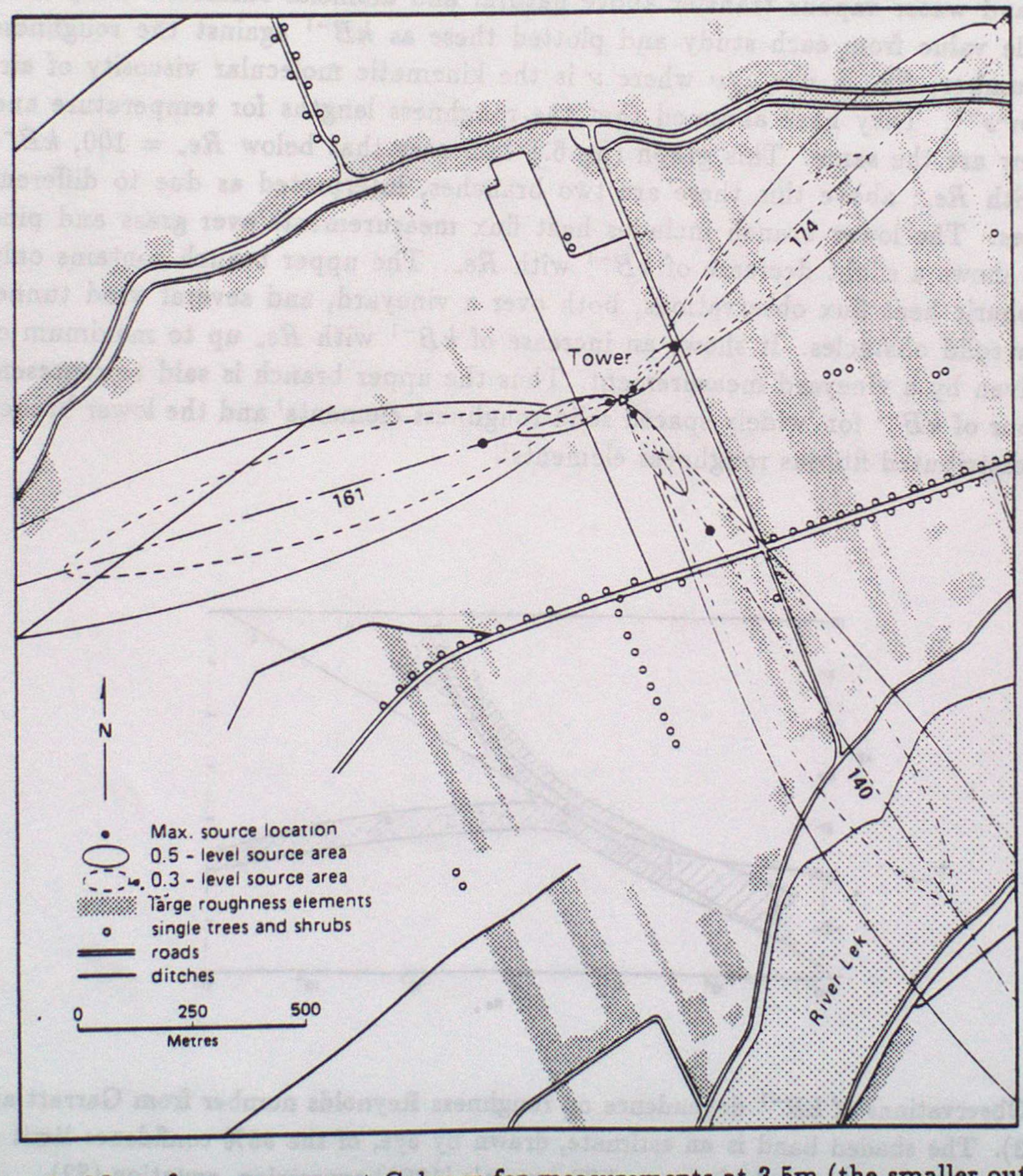

Figure 5. Map of source-areas at Cabauw for measurements at 3.5m (the smaller outlines), and 22.5m (the larger outlines) for wind directions and atmospheric conditions on year days 140, 161 and 174. From Schmid and Oke (1990).

4 Observations and expressions for z_{0t} on a flat, homogeneous surface.

In this section we consider parametrization of z_{0t} i.e. development of expressions for z_{0t} based on available parameters that may be used in numerical weather prediction (NWP). We will see that many of these expressions have been developed in conjunction with results from wind tunnel experiments but it is essential that these results are confirmed by atmospheric observations before we apply them to the NWP models.

4.1 Observations of z_{0t} over flat, homogeneous terrain

Garratt and Hicks (1973) collected atmospheric and wind tunnel observations of momentum, heat and water vapour transfer above natural and artificial surfaces. They then took a single value from each study and plotted these as kB^{-1} against the roughness Reynolds number, $Re_* = u_* z_{0m}/\nu$ where ν is the kinematic molecular viscosity of air, $1.5 \times 10^{-5} m^2 s^{-1}$. They have assumed that the roughness lengths for temperature and water vapour are the same. This graph (fig 6.) indicates that below $Re_* = 100$, kB^{-1} increases with Re_*; above this there are two branches, interpreted as due to different surface types. The lower branch includes heat flux measurements over grass and pine forests and shows a slight decrease of kB^{-1} with Re_*. The upper branch contains only two atmospheric heat flux observations, both over a vineyard, and several wind tunnel studies over solid obstacles. It shows an increase of kB^{-1} with Re_* up to maximum of about 10 given by a vineyard measurement. Thus the upper branch is said to represent the behaviour of kB^{-1} for 'widely spaced solid roughness elements' and the lower branch 'randomly distributed fibrous roughness elements'.

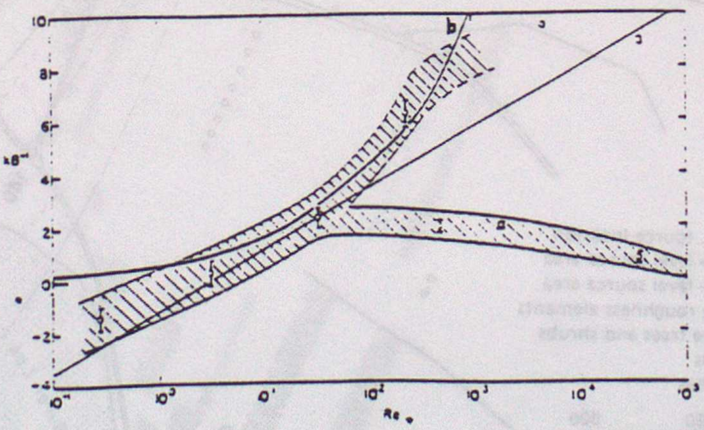

Fig. 6 Observations of kB^{-1} dependence on roughness Reynolds number from Garratt and Hicks (1973). The shaded band is an estimate, drawn by eye, of the 95% confidence limit on this set of observations. Line b is Owen and Thomson's (1963) expression, equation (32).

Observational studies over homogeneous terrain					
Reference	*Site*	z_{0m} (m)	z_{0t} (m)	$\ln \frac{z_{0m}}{z_{0t}}$	$\frac{z_{0m}}{z_{0t}}$
Hicks et al. (1973) from *	Pine forest.			0.5	2
Stewart and Thom (1973) from *	Pine forest.			1.0	3
Rider from *	Short grass.			1.5	4
Hicks from *	Bare soil.			1.6	5
Thom (1972) from *	Bean crop.	0.07	2×10^{-2}	$1.2 - 2.0$	$3 - 7$
Pasquill (from *)	Short grass.			2.4	11
Kohsiek et al. (1993)	La Crau. Flat. Sparse grass and stones;scat -tered 1m stone piles.	0.01	3×10^{-4}	4	40
Graetz (1972) from *	Vineyard;along vines Vineyard;across vines			6 10	500 15,000
Duynkerke (1992)	Cabauw. Flat grass. When $u_* = 0.2$ then When $u_* = 0.6$ then	0.01	 3×10^{-5} 6×10^{-7}	 6 10	 300 10,000
Rider and Robinson (1951)	Kew. Flat grass.	0.002	2×10^{-9}	14	10^6

Table 1. * denotes information from Fig 1. and Table 1. of Garratt and Hicks (1973)

Duynkerke (1992) has calculated z_{0t} from measurements at the Cabauw site in the Netherlands, using observations made in the lower 2m of the atmosphere and at the surface. Measurements were made on three cloudless summer days giving a wide range of heat fluxes (+450 to -50 Wm-2). The 'surface' temperature was determined from grass radiative temperature and the temperature profile on a 2m mast. Stability corrections were ignored because they would be very small at these low measurement heights (see section 2 for stability correction dependence on height).

Figure 7 shows Duynkerke's calculations of roughness length for temperature, z_{0h}. There is large scatter in the data: z_{0t}/z_{0m} varies between about 7 and 2×10^{-8}, z_{0t} varies from approximately 10^{-10} to 10^{-3} Most observation points give z_{0t} as 2-4 orders of magnitude smaller than z_{0m}. The lines indicate a theoretical ratio based on friction velocity and the leaf area index (LAI) (see equation (37)). The estimated LAI of Cabauw is 1.5, and of the shorter grass at Kew (open shapes in figure 7) is 0.58. Thus Duynkerke argues that the data agree well with the theoretical dependence on u_* and LAI.

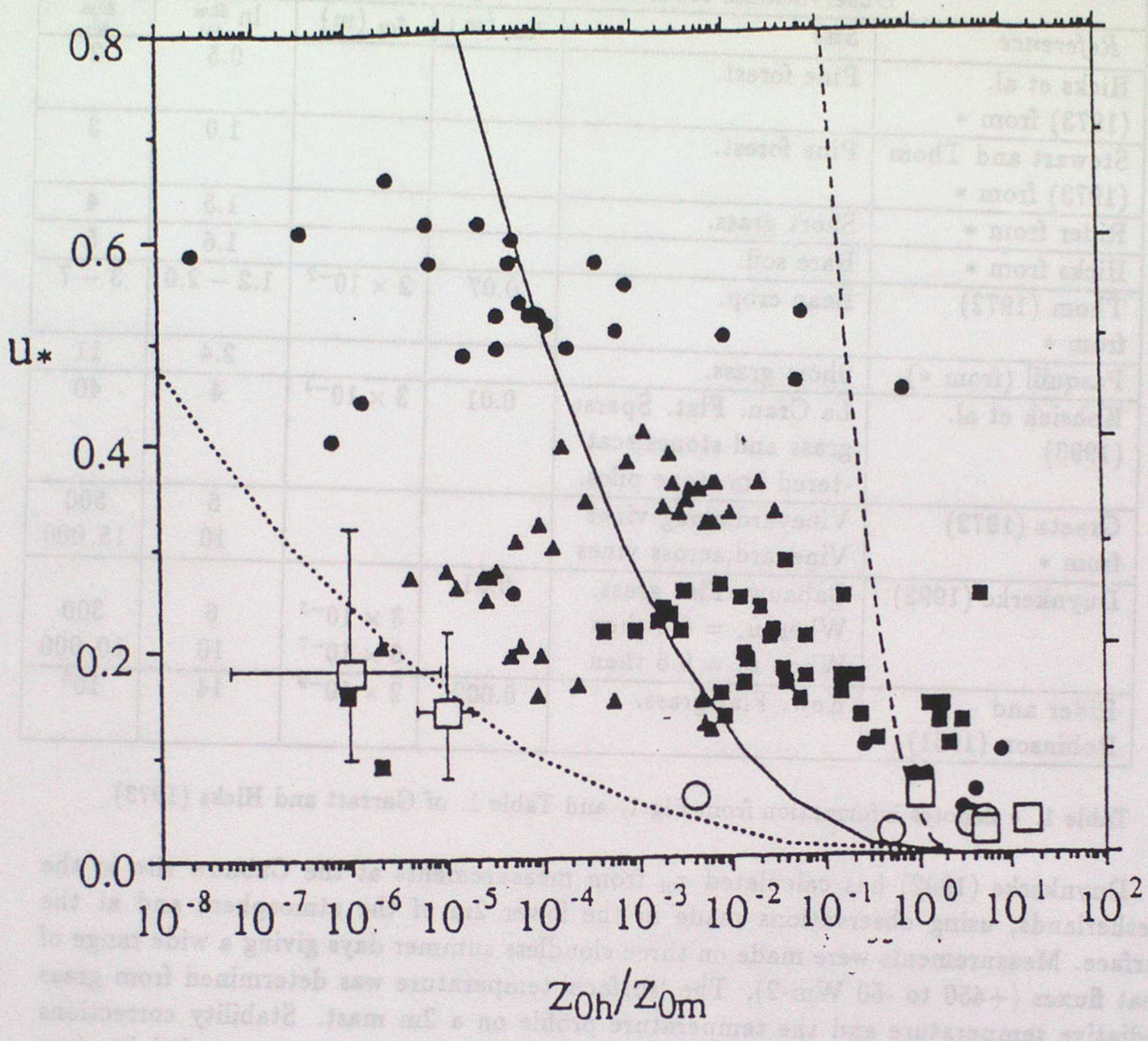

Figure 7. The ratio of roughness lengths for temperature, z_{0h}, to momentum against friction velocity: circles - May 4th; 13 May - squares; 21 July - triangles. Lines are theoretical prediction for different Leaf Area Indices (LAI): $LAI = 0.5$ - short dashed line; $LAI = 1.0$ - solid line; $LAI = 4.0$ - long dashed line. Open shapes indicate observation by Rider and Robinson (1951) at Kew. Duynkerke (1992).

Kohsiek et al. (1993) and De Bruin et al. (1993) report on an observational study in the south of France in an area called La Crau. The interesting characteristic of this flat terrain is the scattered piles of 'bluff bodies' i.e. 1m high piles of stones. Kohsiek et al. have calculated a z_{0t} of $3.3 \times 10^{-4} m$ from measurements of the radiometric surface temperature and 10m temperature, and eddy correlation measurements of momentum and heat fluxes. They then considered the sensitivity of the heat flux to the sublayer Stanton number, B, by calculating the surface sensible heat fluxes from temperature measurements and a range of values for B. The results are shown in Table 2.

Sensitivity of calculated H_s to z_{0t}			
B^{-1}	z_{0t}	z_{0m}	Error in calculated H_s: (calculated H_s) - (observed H_s)
1	8.7×10^{-3}	1.3×10^{-2}	$\approx 100\%$ error when (observed H_s) = $300 Wm^{-2}$
6	1.2×10^{-3}	1.3×10^{-2}	$\approx \pm 20\%$ error when observed $H_s = 300 Wm^{-2}$
9	3.3×10^{-4}	1.3×10^{-2}	0. This is the observed value of z_{0t}.
25	5.9×10^{-7}	1.3×10^{-2}	$\approx -70\%$ error when observed $H_s > 100 Wm^{-2}$

Table 2. Sensitivity of surface sensible heat flux, H_s, calculated from observed temperatures, to z_{0t}. The percentage errors as a fraction of the observed H_s are given. From Kohsiek et al (1993)

Table 2 shows that using a roughness length approximately 3 times that observed, $z_{0t} = 1.2 \times 10^{-3} m$, gave acceptably small errors in calculated sensible heat fluxes (i.e. within $50 Wm^{-2}$ of the actual observed heat flux). But, a z_{0t} 30 times that observed, $z_{0t} = 8.7 \times 10^{-3}$, was unacceptable, giving calculated heat fluxes of $700 Wm^{-2}$ when $300 Wm^{-2}$ was observed. Using a smaller roughness length of $z_{0t} = 5.9 \times 10^{-7}$ typically gave calculated values that were about one third of the observed flux.

In a review of observational studies in 1982, Brutsaert concluded that a reasonable estimate for kB^{-1} over most homogeneous, permeable surfaces was 2, but 1 or smaller should be expected over stands of large trees (Brutsaert (1982), Chapter 4). This is supported by the observational results of Hicks et al. (1973), Stewart and Thom (1973), Rider (from Garratt and Hicks (1973)), Hicks (from Garratt and Hicks (1973)), Thom (1972) and Pasquill (from Garratt and Hicks (1973)). However Duynkerke (1992) and Rider and Robinson (1951) find much higher values of kB^{-1}. Therefore further atmospheric observational studies over homogeneous terrain are needed to resolve the discrepancy.

A possible explanation for the difference in the results over grass surfaces is that Pasquill and Rider both used spirit thermometers to observe the surface temperature, whereas other studies have used a radiometric surface temperature.

4.2 Expressions for z_{0t} over a flat, homogeneous surface from flow and terrain characteristics.

Owen and Thomson (1963) have devised an expression for B^{-1} (see equation (25)) over aerodynamically rough surfaces from theoretical ideas and wind tunnel experiments. A simplified form of this relationship is plotted as line b in figure 6 from Garratt and Hicks (1973).

$$B^{-1} \simeq \frac{0.15}{k}(30Re_*)^{0.45} Pr^{0.8} \tag{32}$$

valid for $10 < Re_* < 10^4$, where $Re_* = u_* z_{0m}/\nu$ is the roughness Reynolds number. Pr, the Prandtl number, is ν divided by the molecular diffusivity for heat $\approx 2.1 \times 10^{-5} m^2 s^{-1}$.

Brutsaert (1975a, 1975b, 1979) has come up with theoretical expressions to fit the upper and lower branches of the Garratt and Hicks (1973) graph. There are a lot of assumptions in this work but it would be useful to have equations for $\ln\left(\frac{z_{0m}}{z_{0t}}\right)$ if observations show that they work.

For permeable roughness elements i.e. the lower branch, Brutsaert (1979) uses a numerical model of turbulent flow in a canopy to formulate heat transfer coefficients and thus determine $\ln(z_{0m}/z_{0t})$ for a variety of surface types. The results show, in agreement with Chamberlain (1966) and Garratt and Hicks (1973), that kB^{-1} for fibrous roughness elements as opposed to bluff roughness elements is relatively insensitive to u_* and independent of z_{0m}. Depending on vegetation type this gives something of the order

$$\ln \frac{z_{0m}}{z_{0t}} = 2 \tag{33}$$

for a wide range of roughness Reynolds number. The model predicts a lower value over aspen forest: $\ln(z_{0m}/z_{0t}) = 0.5$. This theoretical argument is supported by observations over homogeneous terrain in Thom (1972), Hicks et al (1973), Stewart and Thom (1973) and by Rider, Hicks and Pasquill reported in Garratt and Hicks (1973) (see Table 1, section 4.1). Also measurements over heterogeneous terrain described in Garratt (1978) give a value of 2.5 ± 0.5 (see Table 3, section 5.1). However some other experimental studies suggest a much higher value of $\ln(z_{0m}/z_{0t})$ over a homogeneous surface of permeable roughness elements (eg Rider and Robinson (1951), Duynkerke (1992) see Table 1.)

For bluff bodies i.e. the upper branch, Brutsaert (1975a) derives a fit by matching the fluxes at the interface between the layers in a two layer model. In the higher of the two layers the log profile theory is applied to give,

$$\ln \frac{z_{0m}}{z_{0t}} = k(7.3 Re_*^{0.25} Pr^{0.5} - 5) \tag{34}$$

Brutsaert (1979) concludes that this curve is a good fit to observations based on those collected by Garratt and Hicks (1973). There are only two atmospheric observations in that set, both by Graetz (1972), (see Table 1 section 4). Kohsiek et al.'s (1993) measurements over flat stoney terrain with occasional piles of stones fall below the curve described by equation (34). The surface does include some grass cover so the fibrous element effect may also be important to these results.

Subsequently several authors have attempted to scatterplot the results of one observational study on a Garratt and Hicks type graph (see figure 6) to hopefully pick out agreement with Brutsaert's equation (34). Grant and Wood (1993, personal communication) have identified a serious concern about this approach caused by the correlation between the quantities plotted on the axes which are both functions of z_{0m} (Hicks 1981). They have simulated a set of observations by assuming that $T - T_s$, U and $\overline{w'T'}$ can be measured with perfect accuracy and that unique values of z_{0m} and z_{0t} exist but there are sampling errors in the $\overline{u'w'}$ measurements.

$$-\overline{u'w'} = u_*^2 + \epsilon_{\overline{u'w'}} \tag{35}$$

with

$$\epsilon_{\overline{u'w'}} = N\left[0, u_* \sqrt{\frac{14z}{Ut}}\right] \tag{36}$$

where $t = 3600s$, $\epsilon_{\overline{u'w'}}$ is the sampling error in $\overline{u'w'}$ and $N[\mu, \sigma]$ indicates a normally distributed quantity of mean value μ and standard deviation σ.

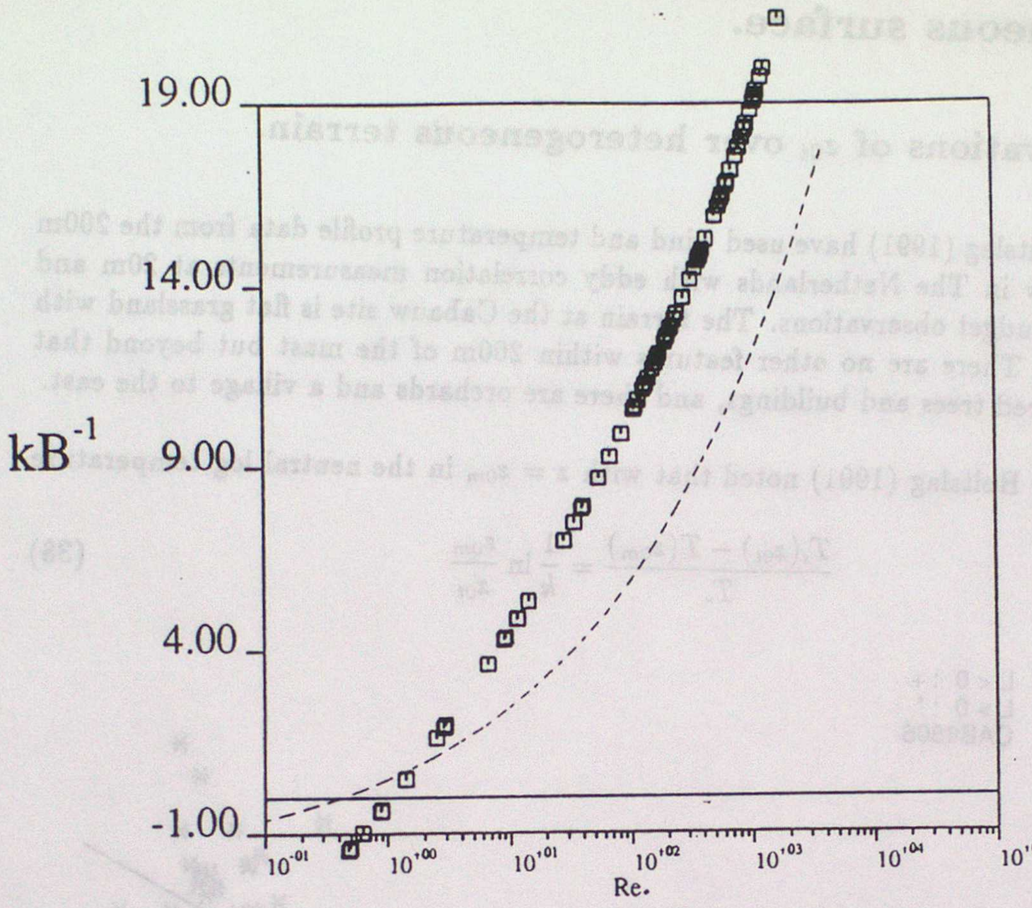

Figure 8. Dependence of kB^{-1} on roughness Reynolds number. The squares are a simulated, single set of observations with a sampling error distribution described by equation (36). The dashed line is the theoretical relationship described by equation (34), (Brutsaert (1975a)).

Figure 8 shows an example of the resulting curves plotted as Re_* against kB^{-1}. So, it is possible to obtain a close fit to the Brutsaert 1975a bluff body curve from sampling errors alone!

Duynkerke (1992) has compared observations over short grass to

$$\ln \frac{z_{0m}}{z_{0t}} = \frac{13u_*^{0.4}}{LAI} - 0.85 \tag{37}$$

where LAI is the leaf area index, or ratio of the total surface area of the leaves to the area of ground beneath them. The results were discussed in section 4.1.

In order to have confidence in any theoretical expression for z_{0t} we need measurements over many surface types. If we can fit simple rules to these observations then we may be able to determine datasets of global z_{0t} due to surface cover, for use in NWP and GCMs, from vegetation/land-use datasets which are currently available.

5 Observations and expressions for z_{0t} on a flat, heterogeneous surface.

5.1 Observations of z_{0t} over heterogeneous terrain.

Beljaars and Holtslag (1991) have used wind and temperature profile data from the 200m mast at Cabauw in The Netherlands with eddy correlation measurements at 20m and surface energy budget observations. The terrain at the Cabauw site is flat grassland with narrow ditches. There are no other features within 200m of the mast but beyond that there are scattered trees and buildings, and there are orchards and a village to the east.

Beljaars and Holtslag (1991) noted that with $z = z_{0m}$ in the neutral log temperature profile we have,

$$\frac{T_s(z_{0t}) - T(z_{0m})}{T_*} = \frac{1}{k} \ln \frac{z_{0m}}{z_{0t}} \tag{38}$$

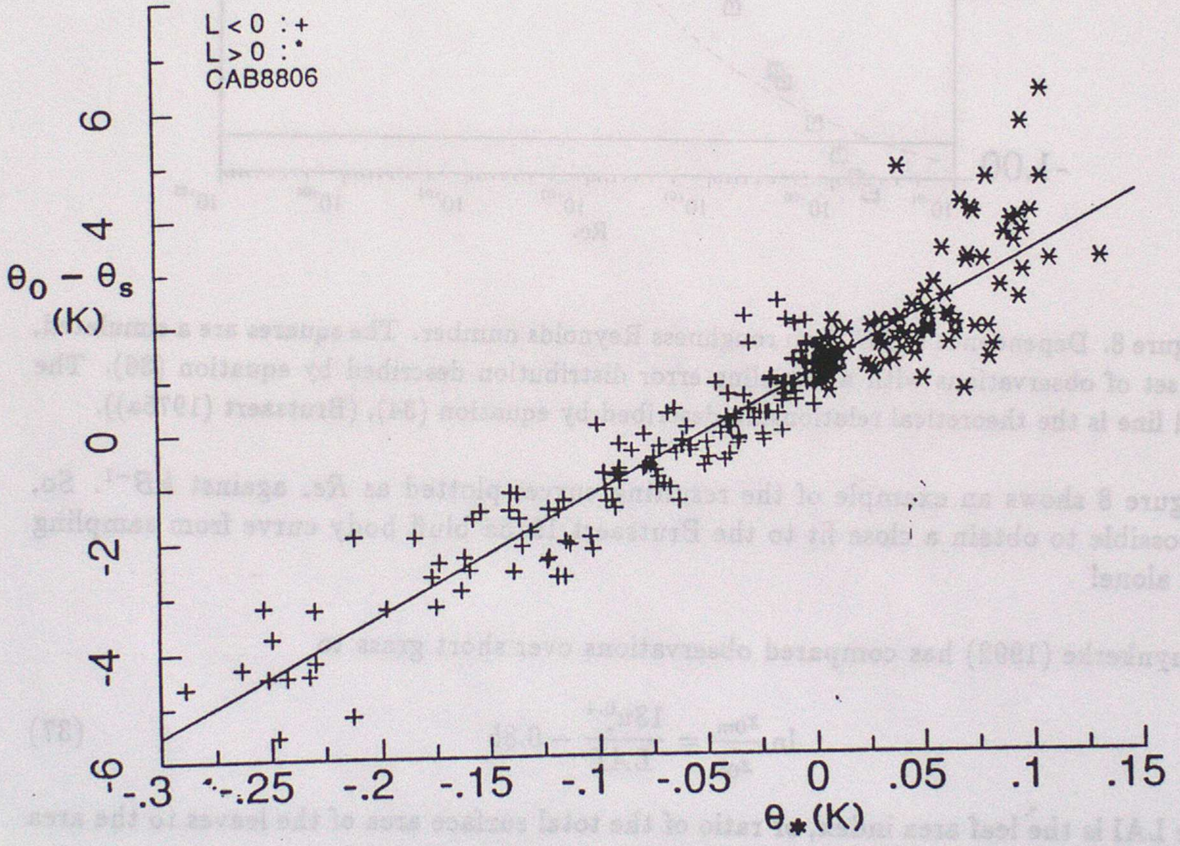

Figure 9. Observations of reference potential temperature, θ_*, against the potential temperature difference between z_{0m} and z_{0t} extrapolated from surface layer observations over grassland with scattered trees and buildings by Beljaars and Holtslag (1991).

Many numerical models (eg UK Met Office Unified Model) assume that $z_{0t} = z_{0m}$, so plotting $T_s(z_{0t}) - T(z_{0m})$ against T_* gives a measure of the error in this assumption and also the gradient of any linear fit will give us B^{-1} as can be seen from equation (25). Figure 9 shows this plot from Beljaars and Holtslag (1991). The temperature difference is as high as $\pm 6K$ and the gradient of the least squares fit gives $B^{-1} = 21.9 \pm 0.6$.

Duynkerke (1992) also took measurements at Cabauw but by taking measurements below 2m considers them to be representative of homogeneous terrain consisting of short grass. So we might expect these two heterogeneous and homogeneous experiments to show different results, but in fact Duynkerke's scattered data suggests B^{-1} in the range $15-25$ which encompasses Beljaars and Holtslag's result.

The observations at Pershore made by the Met. Office Research Unit were over a similar type of terrain to Cabauw. For the purpose of calculating z_{0t}, atmospheric profiles were measured between 16 and 300m with a tethered balloon over an area of flat grass, but there were clumps of trees and buildings approximately 1km away. A Schmid and Oke (1991) source-area analysis suggested that these distant obstacles influenced the measurements. The results obtained were very scattered (z_{0m}/z_{0t} varied between 10 and 10,000) so typical values are quoted in table 3 below.

Observational studies over heterogeneous terrain					
Reference	*Site*	z_{0m} (m)	z_{0t} (m)	$\ln \frac{z_{0m}}{z_{0t}}$	$\frac{z_{0m}}{z_{0t}}$
Garratt (1978)	Flat. Scattered 8m eucalyptus, dry 1m grass and bare sandy soil.	0.4	4×10^{-2}	2.5	12
Hopwood (1993) Personal communication	Pershore. Flat grass. Clumps of trees, isolated buildings.	0.09	4×10^{-4}	6	250
Blyth and Culf (1993)	Tiger-bush, $L = 30m$, $h = 4m$, $d = 0m$, bare soil.		2×10^{-3}	6	≈ 500
Blyth and Culf (1993)	Tiger-bush, $L = 30m$, $h = 4m$, $d = 2m$, bare soil.		2×10^{-4}	9	≈ 5000
Beljaars and Holtslag (1991)	Les Gers. Undulating with amplitude up to 50m wavelength 5km, soil, grass, crops and trees			8	4500
Beljaars and Holtslag (1991)	Cabauw. Flat grass. Isolated trees and buildings	0.01 -0.15	2×10^{-6}	9	6000
Hignett (1993)	Cardington. Flat grass.	0.004	2×10^{-7}	10	20,000

Table 3. Typical values of z_{0m} and z_{0t} over heterogeneous terrain.

Garratt (1978) finds a value of $\ln(z_{0m}/z_{0t})$ over terrain covered by scattered eucalyptus trees, grassland and bare soil (see Table 3) which is smaller than those reported in the other heterogeneous studies and closer to the values in the top half of Table 1 (observations over homogeneous terrain). Garratt's value is also close to Brutsaert's (1979) prediction for permeable roughness elements, $\ln(z_{0m}/z_{0t}) \approx 2$. However, all the other studies find values greater than 2.

The measurements of Blyth and Culf (1993) in HAPEX-Sahel are further evidence for $z_{0t}/z_{0m} < 0.1$ They have found ratios of around 10^{-3} depending on the choice of zero-plane displacement.

5.2 Expressions for area-average z_{0t}.

Area-average fluxes of heat and moisture are desirable quantities for NWP and GCMs, whose grid boxes must typically represent regions that include several surface types (Hewer (1992)). The theory in section 2 is based on the idealised situation of homogeneous terrain. In this section we consider how to extend these theoretical ideas to heterogeneous terrain.

The problem is that the heat flux is diagnosed from a product, and the product of averages is not generally the same as the average of a product , i.e. consider a region divided into fractional areas f_i of different surface types such that,

$$\sum f_i = 1 \tag{39}$$

Each fraction has a local friction velocity and reference temperature u_{*i} and T_{*i}. From the log profile equation (7) and surface sensible heat flux equation (4),

$$H_s = \frac{\rho c_p u_* k(T_s(z_{0t}) - T(z))}{\ln(z/z_{0t})} \tag{40}$$

Now take the area-average, denoted by angled brackets, so that for any quantity A we have, $\langle A \rangle \equiv \sum f_i A_i$ Then,

$$\langle H_s \rangle = \langle \frac{\rho c_p u_* k(T_s(z_{0t}) - T(z))}{\ln(z/z_{0t})} \rangle \neq \frac{\rho c_p k \langle u_* \rangle \langle T_s(z_{0t}) - T(z) \rangle}{\ln(z/\langle z_{0t} \rangle)} \tag{41}$$

So, if we try to diagnose the area-averaged sensible heat flux from an area-averaged friction velocity, temperature and roughness length for temperature we will not get the right answer!

Vihma and Savijärvi (1991) have summarised published techniques for averaging roughness lengths for momentum, which we may consider as possible approaches for z_{0t}. We call these average values the effective roughness length for temperature, z_{0t}^{eff}, by whichever method they are derived. They have the following forms:

1. simple logarithmic average,
   $\ln(z_{0m}^{eff}) = \langle \ln(z_{0m}) \rangle$
2. area-average surface stress from the lowest model level wind,
   $U(z_1) = (< u_*^2 >^{1/2} / k) \ln(z_1 / z_{0m}^{eff})$
   Fiedler and Panofsky (1962)
3. area-average geostrophic drag coefficient,
   Smith and Carson (1977)
4. weighted local drag coefficients,
   Divide surface into identifiable terrain types and fit weighted sum of local drag coefficients to reproduce observed average,
   van Dop (1983), Kondo and Yamazawa (1986)

5. average drag coefficients at the height of the lowest model level, z_1,
$(\ln z_1/z_{0m}^{eff})^{-2} = \langle(\ln z_1/z_{0m})^{-2}\rangle$
van Dop (1983) and Wieringa (1986)

6. average drag coefficients at the 'blending height' l_b,
$[\ln(l_b/z_{0m}^{eff})]^{-2} = \langle[\ln(l_b/z_{0m})]^{-2}\rangle$ typically $l_b = L/200$ where L is the horizontal length scale of the roughness patch,
Mason (1988)

7. average at the lowest model level
$(\ln z_1/z_{0m}^{eff})^{-1} = \langle(\ln z_1/z_{0m})^{-1}\rangle$
Andre and Blondin (1986)

8. add the variance of $\ln z_{0m}$ to the simple log average,
$\ln(z_{0m}^{eff}) = \langle\ln(z_{0m})\rangle + 0.09(\langle(\ln z_{0m})^2\rangle - \langle\ln z_{0m}\rangle^2)$ where 0.09 is derived from Rossby number similarity theory (Taylor (1987))

The simple log average gives the smallest value of all these methods. Its easy to calculate and is probably a good approximation for type B heterogeneity (Shuttleworth (1988)), i.e. when the horizontal scale of surface type variation is greater than 10 km, see Fig. 10. In this case there will be a separately identifiable boundary layer over each terrain type. The more interesting case is for the type A, patchy land surface cover (see Fig. 10) where only the lower part of the boundary layer is directly modified by the local surface type.

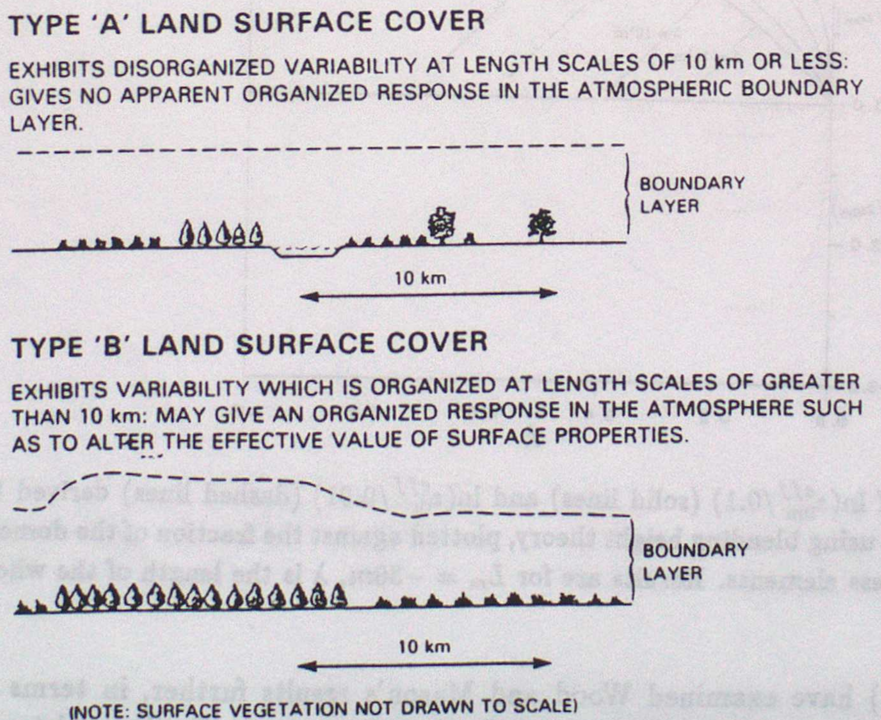

Figure 10. Surface type classification from Shuttleworth (1988).

Item 6 above (Mason (1988)) is the only method with a dependence on the length scale of the roughness variation so that for the other methods the same fractional coverage would give the same effective roughness length whether organised into small clumps or in one contained area.

Since Vihma and Savijärvi's review (1991), Wood and Mason (1991) have defined an effective roughness length for temperature by eliminating surface temperature from the log temperature profile equation evaluated at the blending height (see section 5.2.1) and assuming a constant surface sensible heat flux. They have then applied this definition to a domain, length λ metres, which consists of two surface types, with roughness lengths for temperature of 0.1m and 0.001m and roughness lengths for momentum of 1.0m and 0.01m. Figure 11 shows the variation of the effective roughness lengths for temperature (dashed lines) and momentum (solid lines) with fraction of the surface with a high roughness length. The effective roughness lengths are scaled with a simple logarithmic average and plotted as their log_{10}. For example in the case of the z_{0t}^{eff} the ordinate is $log_{10}(z_{0t}^{eff}/z_{0tm})$ where $z_{0tm} = 0.01m$ is a log average of the high and low roughness length. The effective roughness length for temperature decreases as the fraction of rougher surface increases from 0.0 to ≈ 0.2. So the effective value is initially lower than that of the smoothest surface; it then increases rapidly with increasing fraction of rougher surface. Contrary to averaging a roughness length for momentum, the effective roughness length for temperature is dominated by the smooth elements.

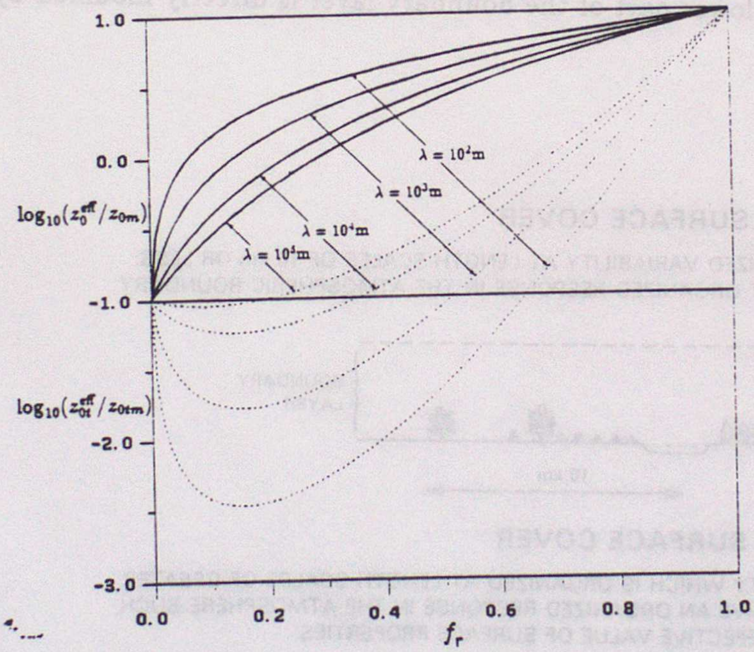

Figure 11. Values of $\ln(z_{0m}^{eff}/0.1)$ (solid lines) and $\ln(z_{0t}^{eff}/0.01)$ (dashed lines) derived by Wood and Mason (1991) using blending height theory, plotted against the fraction of the domain covered by large roughness elements. Results are for $L_m = -30m$, λ is the length of the whole domain.

Blyth et al. (1993) have examined Wood and Mason's results further, in terms of resistances defined by equation (24). They conclude that the correct effective resistance to any flux, F (eg H_s), is

$$r_a^{eff} = \frac{\sum F_i r_{ai}}{\sum F_i} \qquad (42)$$

Thus for momentum,

$$r_{am}^{eff} = \frac{\sum u_{*i}^2 r_{ami}}{\sum u_{*i}^2} \qquad (43)$$

and since by definition $r_{ami} \equiv U/u_{*i}^2$, and making the assumption of a homogeneous wind at the blending height:

$$\frac{1}{r_{am}^{eff}} = \langle \frac{1}{r_{am}} \rangle \qquad (44)$$

This is like calculating the effective resistance of parallel resistors in an electrical circuit and it means that the smallest resistance (or largest roughness lengths) dominates the averaging. Algebraically this is the same as obtained by Mason (1988) and Wood and Mason (1991) and is illustrated by the solid lines in Figure 11. For heat,

$$r_{ah}^{eff} = \frac{\sum u_{*i} T_{*i} r_{ahi}}{\sum u_{*i} T_{*i}} \qquad (45)$$

and making Wood and Mason's crucial assumption of a constant heat flux which means a constant $u_* T_*$ then

$$r_{ah}^{eff} = \langle r_{ah} \rangle \qquad (46)$$

This is like calculating the effective resistance of series resistors in an electrical circuit and it means that the larger resistance (or smaller roughness length) is more important, as shown by the dashed lines in Figure 11 from Wood and Mason (1991).

Lhomme (1992) has devised 'omega averaging' coefficients by eliminating the surface sensible heat flux from the surface energy balance equation (29) and equation (22) to give an expression for the surface temperature. By assuming that the correct average surface temperature is given by a simple area-average, and after some algebra,

$$\frac{1}{r_{ah}^{eff}} = \frac{\sum \frac{f_i \omega_i}{r_{ahi}}}{\sum f_i \omega_i} \qquad (47)$$

where

$$\omega \equiv \frac{1}{\frac{1}{r_0} + \frac{1}{r_{ah}} + \frac{s}{\gamma(r_{am} + r_s)}} \qquad (48)$$

and r_0 is a notional resistance to radiative transfer, γ is the psychrometric constant ≈ 0.0004 grammes of water per gramme of air K^{-1}. This method also suggests that the effective roughness length for temperature is weighted towards the smaller roughness lengths (larger resistances). Further details of Lhomme's modelling results will be given in section 7.

5.2.1 Blending height

The concept of a blending height was first proposed by Wieringa (1976,1986) for calculating climatological, area-mean winds from standard 10m mast observations and has since been used to evaluate an effective roughness length (Mason (1988), Claussen (1990)). The idea is that over flat, patchy or type A terrain the wind profile is in equilibrium with the local roughness elements near the surface, but responds to a wider area higher up. So, if we consider the example of flat grassland with occasional groups of trees, then in the surface layer above the grass we expect the wind profile to follow the log relationship with $u_* = u_*^{grass}$ and $z_{0m} = z_{0m}^{grass}$, and in the surface layer above the trees the wind profile would be defined by, $u_* = u_*^{trees}$ and $z_{0m} = z_{0m}^{trees}$.

$$U(grass, z) = \frac{u_*^{grass}}{k} \ln(\frac{z}{z_{0m}^{grass}}) \qquad U(trees, z) = \frac{u_*^{trees}}{k} \ln(\frac{z}{z_{0m}^{trees}})$$

Higher up in the boundary layer, the wind field would be homogeneous, i.e. the wind would be the same above grass or trees.

$$U(x, z) = U_{upper}(z) \tag{49}$$

Now we define an *effective roughness length for momentum* to give us the area-average surface stress from the homogeneous upper wind. So in neutral conditions,

$$U_{upper}(z) = \frac{< u_*^2 >^{1/2}}{k} \ln\left(\frac{z}{z_{0m}^{eff}}\right) \tag{50}$$

where angled brackets denotes an area-averaged quantity. The *blending height*, $z = l_b$ is a theoretical height at which both local equilibrium and horizontal homogeneity are approximately satisfied. The area-average surface stress is defined by the upper logarithmic wind profile, equation (50) and also by the area-average from the local logarithmic wind profiles.

$$\frac{k^2 U_{upper}^2(l_b)}{\ln^2 \frac{l_b}{z_{0m}^{eff}}} = \frac{f_{grass} k^2 U^2(grass, l_b)}{\ln^2\left(\frac{l_b}{z_{0m}^{grass}}\right)} + \frac{f_{trees} k^2 U^2(trees, l_b)}{\ln^2\left(\frac{l_b}{z_{0m}^{trees}}\right)} \tag{51}$$

where the f s are the fraction of surface covered by each vegetation type (see equation (39)). Now, if we further assume that equation (49) holds at $z = l_b$,

$$U_{upper}^2(l_b) \simeq U^2(grass, l_b) \simeq U^2(trees, l_b) \tag{52}$$

then equation (51) is reduced to an average of drag coefficients,

$$C_{DN}^{eff}(l_b) = f_{grass} C_{DN}^{grass}(l_b) + f_{trees} C_{DN}^{trees}(l_b) \tag{53}$$

Or, cancelling von Kármán's constant,

$$\frac{1}{\ln^2\left(\frac{l_b}{z_{0m}^{eff}}\right)} = \frac{f_{grass}}{\ln^2\left(\frac{l_b}{z_{0m}^{grass}}\right)} + \frac{f_{trees}}{\ln^2\left(\frac{l_b}{z_{0m}^{trees}}\right)} \tag{54}$$

Thus we can derive z_{0m}^{eff} from z_{0m}^{grass}, z_{0m}^{trees} and l_b.

Mason(1988) showed that the blending height for terrain cover characterized by a horizontal length scale, L, was

$$l_b \simeq \left(\frac{u_*}{U(l_b)}\right)^2 \frac{L}{\pi} \tag{55}$$

which may typically be approximated by,

$$l_b \simeq L/200 \tag{56}$$

Subsequently Wood and Mason (1991) have developed the concept of blending height for temperature and with linear analysis derived,

$$l_{bh} \simeq \left| \frac{LH_s}{U\theta\pi} \right| \tag{57}$$

If $z_{0m} = z_{0t}$ then l_b is of the same order as l_{bh}.

Consistent with this approach, other workers (eg Beljaars and Holtslag (1991)) have found that the effective heat transfer coefficient is mainly due to the dominant surface cover. So if $f_{grass} > f_{trees}$ then

$$C_{HN}^{eff}(l_b) \simeq C_{HN}^{grass}(l_b) \tag{58}$$

If we also define,

$$C_{HN}^{eff}(l_b) = \frac{k^2}{\ln\left(\frac{l_b}{z_{0m}^{eff}}\right) \ln\left(\frac{l_b}{z_{0t}^{eff}}\right)} \tag{59}$$

then

$$\ln\left(\frac{l_b}{z_{0t}^{eff}}\right) = \frac{\ln\left(\frac{l_b}{z_{0m}^{grass}}\right) \ln\left(\frac{l_b}{z_{0t}^{grass}}\right)}{\ln\left(\frac{l_b}{z_{0m}^{eff}}\right)} \tag{60}$$

(Beljaars and Holtslag (1991))

Equation (59) shows that to satisfy equation (58) z_{0t}^{eff} must decrease to compensate for the increase in z_{0m}^{eff}. Beljaars and Holtslag (1991) have used equation (60) to calculate z_{0t}^{eff} for varying ratios of z_{0m}^{eff} to z_{0m}^{grass}. They assume that z_{0t}^{grass} / $z_{0m}^{grass} = 0.1$ (Brutsaert (1982), Garratt and Hicks (1973)) and $l_b = 20m$. Their Table 1 is reproduced below, with additional columns of neutral drag and heat transfer coefficients.

Effective roughness length for temperature from equation (60)					
z_{0m}^{eff}	z_{0m}^{grass}	z_{0m}^{eff} / z_{0t}^{eff}	z_{0t}^{eff}	$C_{DN}^{eff}(20m)$	$C_{HN}^{eff}(20m)$
0.01	0.01	1.0×10^{1}	1.0×10^{-3}	2.8×10^{-3}	2.13×10^{-3}
0.02	0.01	5.4×10^{1}	3.7×10^{-3}	3.4×10^{-4}	2.13×10^{-3}
0.05	0.01	7.2×10^{2}	7.0×10^{-5}	2.8×10^{-3}	2.13×10^{-3}
0.10	0.01	7.4×10^{3}	1.4×10^{-5}	5.7×10^{-3}	2.13×10^{-3}
0.20	0.01	1.3×10^{5}	1.6×10^{-6}	7.5×10^{-3}	2.13×10^{-3}
1.00	0.01	4.1×10^{9}	2.4×10^{-10}	17.8×10^{-3}	2.12×10^{-3}

Table 4. Effective roughness lengths for temperature z_{0t}^{eff} for a varying ratio of the local to effective roughness lengths for momentum z_{0m}^{eff} / z_{0m}. The blending height is taken to be 20 metres, and z_{0t} is assumed to be one tenth of z_{0m}. Calculated from equation (60), after Beljaars and Holtslag (1991).

An effective roughness length for momentum of 0.1m is appropriate for the Cabauw site where the Beljaars and Holtslag data was collected, and the dominant surface cover is short grass, $z_{0m} \approx 0.01$m. The measured ratio of z_{0m}^{eff} / z_{0t}^{eff} was 6.4×10^{3} which is in close agreement with the theoretical calculation of 7.4×10^{3}.

6 z_{0t} for complex terrain

Orography is a further complication in determining a roughness length for temperature, but very little work has been published in this area. The results from two observational studies are summarized in table 5 below.

Observational studies over complex terrain						
Reference	*Site*	z_{0m} (m)	z_{0t} (m)	$\ln \frac{z_{0m}}{z_{0t}}$	$\frac{z_{0m}}{z_{0t}}$
Sugita and Brutsaert (1990)	Kansas hilly prairie, $d = 26.9m$. Undulating with amplitude $\approx$ 50m	1.05 Autumn Spring	 1×10^{-2} 5×10^{-7}	 5 15	 10^2 10^6
Beljaars and Holtslag (1991)	Les Gers. Undulating with amplitude up to 50m wavelength 5km, soil, grass, crops and trees			8	4500

Table 5. Observational studies over complex terrain.

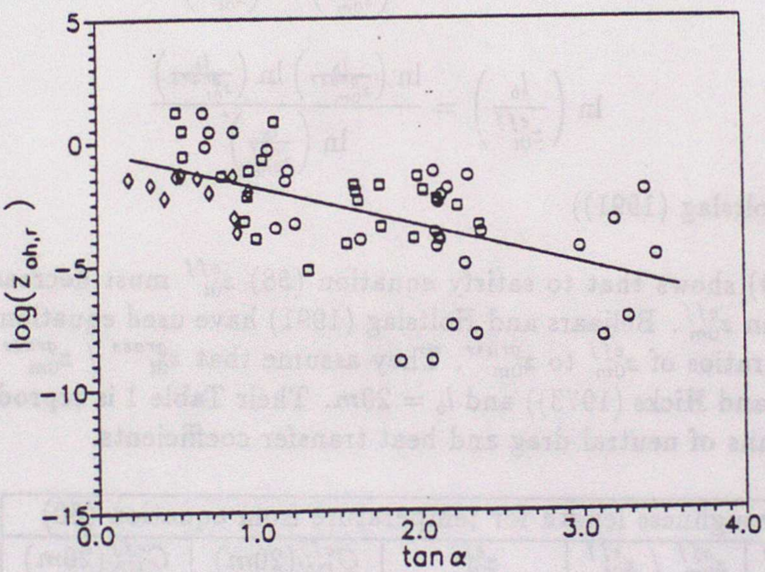

Figure 12 Scatterplot of roughness length for temperature data from Sugita and Brutsaert(1990). The ordinate is log_{10} of the roughness length for temperature derived from a radiometric surface temperature, $z_{0h,r}$. The abscissa is the tangent of solar elevation angle, α.

Sugita and Brutsaert (1990) conducted a field experiment over hilly prairie in Kansas which had a roughness length for momentum of 1.05m and displacement height of 26.9m. The vegetation cover was mainly short grass with perennial trees in the valley bottoms. Over rougher terrain the logarithmic profile is valid in a higher layer and so radiosonde measurements were made between 70 and 140m and Businger-Dyer stability correction functions applied to the log profile theory. The 'surface' temperatures were measured with radiometers. The resulting z_{0t}s are scatterplotted against solar elevation in Figure 12. A very wide range of values was calculated (cf figure 7) from 10^{-16} to 10^{1} (natural log z_{0t} from -37 to +2). Regression analysis leads to a good fit to the solar elevation. It is not clear whether measurements of T_s have allowed for the dependence of the radiometer measurement on its position relative to the solar elevation (see Kustas et al. (1989)). However Verhoef and De Bruin(1993) presented results that also showed a strong dependence on time of day but were not able to say whether this corresponded to variation in, say, wind speed, geostrophic wind, or other factors. The fit of the Sugita and Brutsaert data is slightly improved by including LAI in the regression formula. The observations here were made from May to October so LAI varies and z_{0t} after quality control were calculated to vary from, z_{0t}(spring) = 4.56 $\times 10^{-7}$ (LAI 1.1) to z_{0t}(autumn) = 1.01 $\times 10^{-2}$ (LAI 0.3).

The entry in table 5 from Beljaars and Holtslag (1991) is based on a single observation from the experiment at Les Gers. The measurements at Cabauw reported in the same paper give a ratio of z_{0m}/z_{0t} close to this (see table 3), despite the fact that the terrain there is flat.

7 Modelling Studies

The validity of any assumptions about z_{0t}^{eff} can only be verified by observations but it would be extremely expensive to do experiments over the many surface types and in all the conditions of interest. Therefore it is sensible to combine observational evidence with results from process models.

Wood and Mason (1991) and Lhomme (1992) have conducted modelling studies into type A heterogeneous terrain.

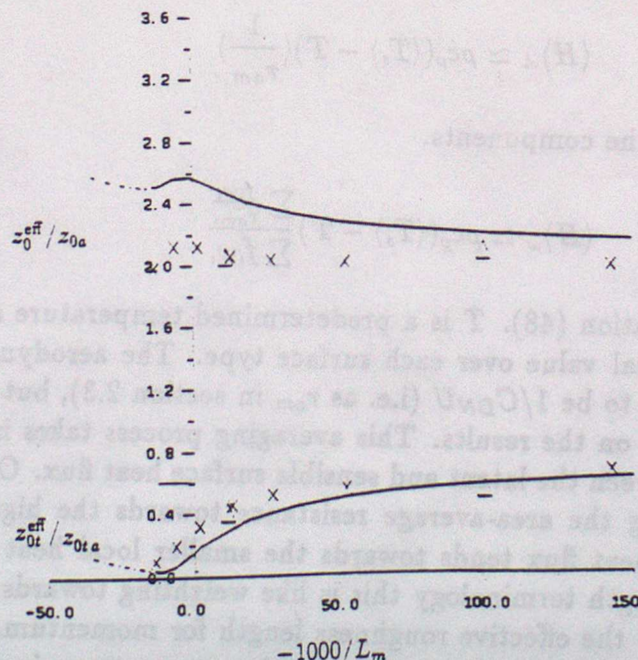

Figure 13. Variation of roughness lengths for momentum (upper line and symbols) and temperature (lower line and symbols) with stability. The crosses are the numerical model results using Businger-Dyer similarity profiles, the triangles are the model with KEYPS similarity profiles. The lines are theoretical results using blending height ideas,(Wood and Mason (1991)).

Wood and Mason (1991) have used a two-dimensional numerical model of the atmospheric boundary layer with a constant surface sensible heat flux lower boundary condition. The model surface is flat but allows spatial variation in the roughness lengths for momentum and temperature. From the numerical model results area-average quantities can be calculated. The effective roughness length for momentum and the effective roughness length for temperature were evaluated from data at 18m, since they were found to be nearly independent of height between 5 and 35m. Figure 13 shows the variation of the effective roughness lengths with stability for a severe sinusoidal variation in the logarithm of roughness lengths. The crosses and triangles are model results and the continuous lines were derived from blending height theory. The roughness length for momentum is written without an 'm' subscript in this figure. The effective roughness lengths are normalised by the logarithmic average, z_{0ta} (item 1, section 5.2) so that $\ln z_{0ta} = \langle \ln z_{0t}(x) \rangle$. For the purposes of comparison the local roughness lengths were set to the same values, i.e. $z_{0t}(x) = z_{0m}(x)$. Thus it can be seen from figure 13 that while z_{0m}^{eff} is typically twice the logarithmic average value, z_{0t}^{eff} is less than half the logarithmic average. The model results show little variation of z_{0m}^{eff} with stability and the theoretical line only varies between 2.2 and 2.5 times the log average. Wood and Mason conclude that this variation would not be significant to numerical modelling parametrization schemes. z_{0t}^{eff}, however varies between one half and one twentieth of the log average value z_{0ta}, with a rapid change occurring near neutral stability i.e. $-1000/L_m = 0.0$. This relationship requires further investigation.

Lhomme (1992) devised a method of 'omega averaging' the local values of resistance , r_{ah}, albedo, α, ground flux, G, and the resistance for evaporation $r_{ah} + r_s$ by eliminating the surface sensible heat flux from the surface energy budget equation (29) and equation (22). For the case of a region divided into two surface types covering equal areas (eg forest and lake), a numerical model was used to calculate the local fluxes over each surface and thus the model area-average was derived. The model average fluxes, $\langle H \rangle$, were compared with those calculated by simple area averaging of the components (eg resistance)

$$\langle H \rangle_A \simeq \rho c_p(\langle T_s \rangle - T)\langle \frac{1}{r_{am}} \rangle \tag{61}$$

and also omega averaging the components.

$$\langle H \rangle_\omega \simeq \rho c_p(\langle T_s \rangle - T)\frac{\sum \frac{f_i \omega_i}{r_{ami}}}{\sum f_i \omega_i} \tag{62}$$

where ω is defined by equation (48). T is a predetermined temperature at 30m and the subscript i denotes the local value over each surface type. The aerodynamic resistance r_{ah} is defined in this study to be $1/C_{DN}U$ (i.e. as r_{am} in section 2.3), but this should not have any qualitative effect on the results. This averaging process takes into account the partitioning of energy between the latent and sensible surface heat flux. Omega averaging has the effect of weighting the area-average resistance towards the higher local value, so that the area-average heat flux tends towards the smaller local heat flux of the two subareas. In roughness length terminology this is like weighting towards the least rough patches i.e the opposite to the effective roughness length for momentum. The numerical model was run for three pairs of surface types and the omega averaging method always gave an area-average surface sensible heat flux closer to the model average than the simple area-average method.

8 Discussion

The main motivation for the present study is to provide advice to the Unified Model project. Therefore the sensitivity of the Unified Model to variation in z_{0t} is of particular interest. The Single Column version of the Unified Model (SCM, Lean (1992)) was run in a series of five day tests, each with different combinations of z_{0t} and z_{0m} (see Table 6). The UM currently uses $z_{0t} = z_{0m}$ in operational forecast model mode and climate mode, but $z_{0t} = z_{0m}/10$ in mesoscale mode, but atmospheric observations have reported values as low as $z_{0t} = z_{0m}/20,000$ (see section 5.1). SCM was run at climate resolution i.e. 20 vertical levels, the lowest five are at 58, 252, 657, 1231 and 2009 m. Initial data was taken from measurements on a cloudless summer day at the Met Office Research Unit, Cardington. The Cardington data included wind, temperature and humidity profiles, surface temperature, surface pressure, screen temperature and cloud cover for 1100 on 19/7/90 (year-day 198). The model also requires initial soil moisture content and deep soil temperatures: estimates of these quantities were tuned to give the best model-predicted surface sensible heat flux for the roughness lengths of Run 2. Table 6 shows the response of SCM to the initial conditions after one timestep. Although it has accurate screen temperatures it was not capable of maintaining the high surface temperature that was observed. The model screen temperature is determined largely by the boundary layer temperature profile which was initialised to observed values but the model surface temperature depends more critically on the model's surface energy balance and z_{0t}. The model does not seem capable of simulating steep low level temperature gradients for any value of z_{0t}. This may be due to the simple representation of the vegetative canopy. However, we seek to demonstrate the sensitivity of SCM to z_{0t}.

Single Column Unified Model response to initial conditions							
	Run 1	Run 2	Run 3	Run 4	Run 5	Run 6	Observations
z_{0t} m	0.02	0.002	0.2	0.02	0.002	0.0002	
z_{0m} m	0.02	0.02	0.2	0.2	0.2	0.2	≈ 0.1
T_s K	309.7	310.0	308.8	309.3	309.6	309.8	317.6
$T_{1.5}$ K	299.8	299.0	302.6	299.9	299.1	298.9	299.8
H_s Wm^{-2}	129.9	138.4	86.6	112.9	125.9	133.5	135.8

Table 6. Surface temperature, T_s, screen temperature, $T_{1.5}$, and surface sensible heat flux, H_s, produced after one timestep and as observed.

The results showed that decreasing z_{0t} increases the daily maximum surface temperature. The most extreme case of this is seen by comparing run 3 with run 6. Figures 14 and 15 show timeseries of surface temperature, screen temperature, surface sensible heat flux and soil heat flux for these two runs. For run 6, $z_{0t} \times 1000 = z_{0m} = 0.2$, the maximum surface temperature is typically 2K higher than for run 3, $z_{0t} = z_{0m} = 0.2$. The minimum surface temperature differs by less than 1K. The values of screen temperatures are very similar in the two runs but the run 6 temperature cycle lags the run 3 cycle by a radiation timestep which is 3 hours. The model has a tendency to develop excessive cloud, these runs are no exception to that and they both rain from year-day 201 onwards.

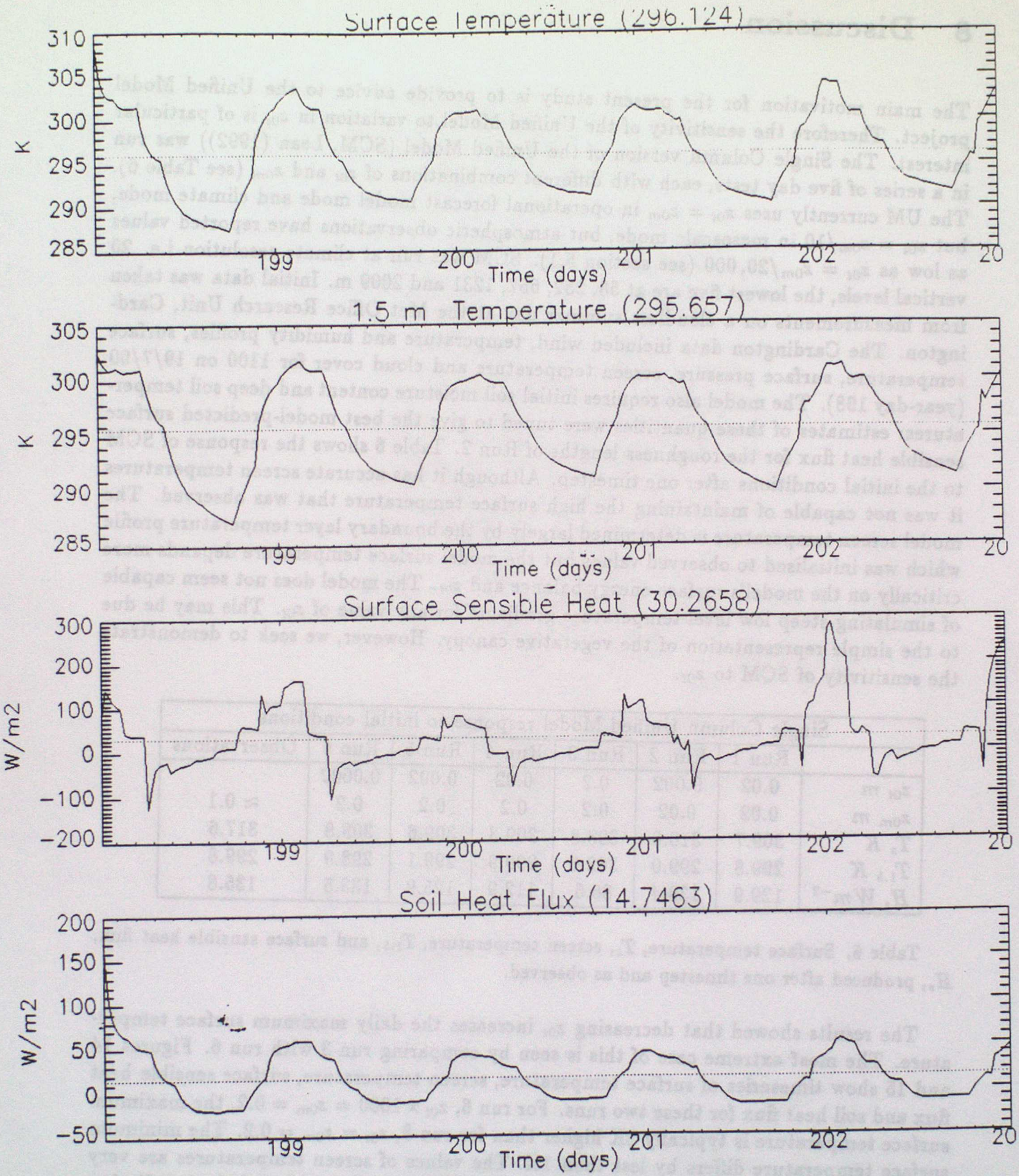

Figure 14. Timeseries from run 3 of the Single Column Unified Model. $z_{0t} = z_{0m} = 0.2$. A 5 day run from 1100 on year-day 198.

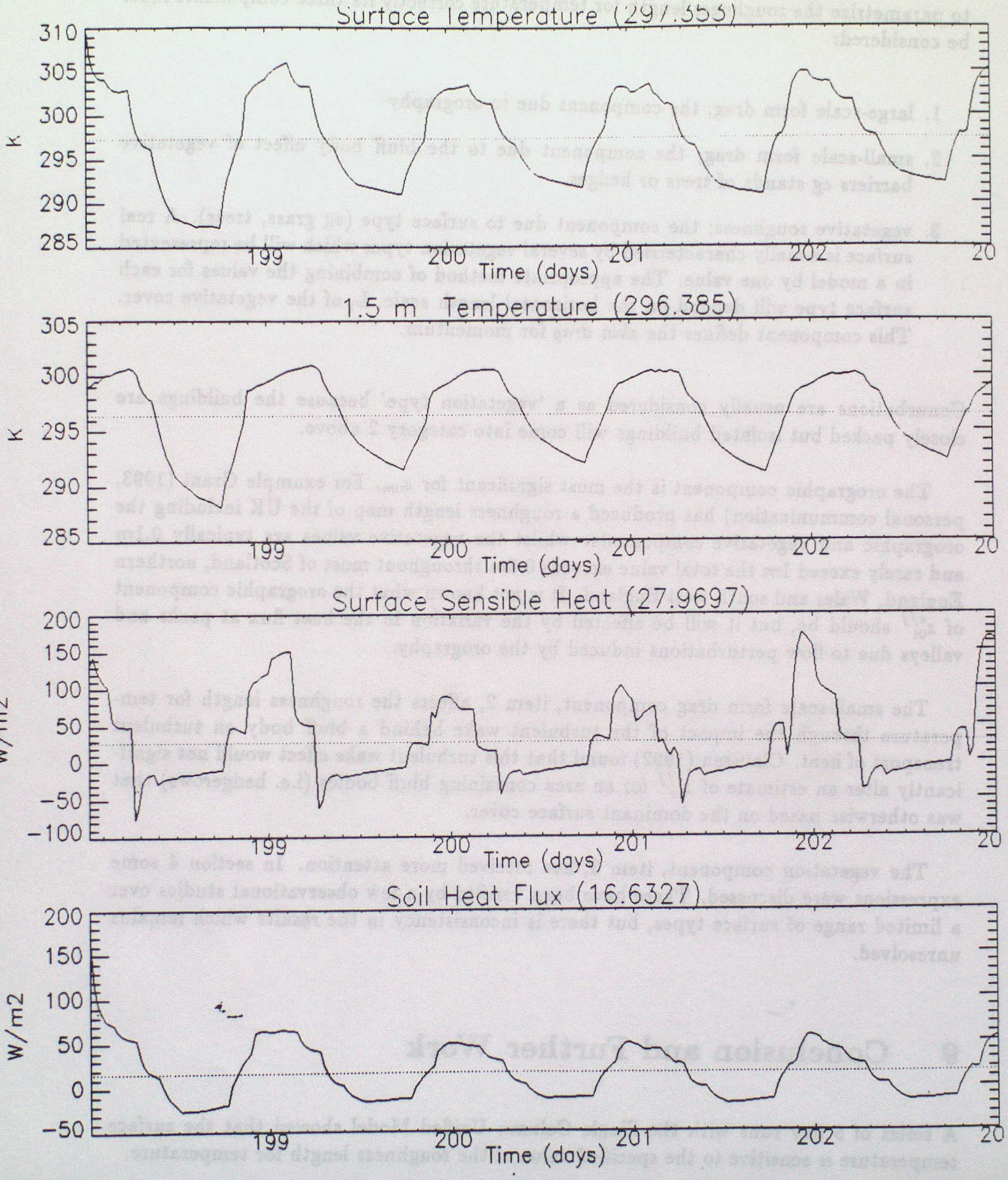

Figure 15. Timeseries from run 6 of the Single Column Unified Model. $z_{0t}\times 1000 = z_{0m} = 0.2$. A 5 day run from 1100 on year-day 198.

These results suggest that the Unified Model is sensitive to the value of z_{0t}. In order to parametrize the roughness length for temperature correctly its three components must be considered:

1. large-scale form drag; the component due to orography
2. small-scale form drag; the component due to the bluff body effect of vegetative barriers eg stands of trees or hedges.
3. vegetative roughness; the component due to surface type (eg grass, trees). A real surface is usually characterised by several vegetation types which will be represented in a model by one value. The appropriate method of combining the values for each surface type will depend on the horizontal length scale, L, of the vegetative cover. This component defines the *skin drag* for momentum.

Conurbations are usually considered as a 'vegetation type' because the buildings are closely packed but isolated buildings will come into category 2 above.

The orographic component is the most significant for z_{0m}. For example Grant (1993, personal communication) has produced a roughness length map of the UK including the orographic and vegetative components: whilst the vegetative values are typically $0.1m$ and rarely exceed $1m$ the total value exceeds $0.5m$ throughout most of Scotland, northern England, Wales and south west England. It is not known what the orographic component of z_{0t}^{eff} should be, but it will be effected by the variation in the heat flux at peaks and valleys due to flow perturbations induced by the orography.

The small-scale form drag component, item 2, affects the roughness length for temperature through the impact of the turbulent wake behind a bluff body on turbulent transport of heat. Claussen (1992) found that this turbulent wake effect would not significantly alter an estimate of z_{0t}^{eff} for an area containing bluff bodies (i.e. hedgerows) that was otherwise based on the dominant surface cover.

The vegetation component, item 3, has received more attention. In section 4 some expressions were discussed. These have been verified by a few observational studies over a limited range of surface types, but there is inconsistency in the results which remains unresolved.

9 Conclusion and Further Work

A series of 5 day runs with the Single Column Unified Model showed that the surface temperature is sensitive to the specified value of the roughness length for temperature.

The roughness length for temperature appropriate for use in GCMs is at least an order of magnitude smaller than the roughness length for momentum. Unlike z_{0m}^{eff}, z_{0t}^{eff} is mainly determined by the surface with the largest fractional cover, rather than low fractions of rougher surfaces (eg equation (60)). So, for example, the roughness length for temperature of an area of grass and isolated trees would almost be the same as that for the grass. This must be because the turbulent transport of heat is only affected in a small area by isolated obstacles. If, however, we have a surface with more equal proportions of rough and smooth surfaces then an averaging technique is required.

Roughness length for temperature is a difficult quantity to measure over real surfaces because accurate temperature measurements are required. Wood and Mason (1991) also find it to be a stability dependent quantity which is a further complication that is not well understood. There are insufficient observational results available in the literature to confirm theoretical results.

Very little is known about z_{0t} over hilly terrain.

10 Acknowledgements

Many of the ideas and organisation of my thoughts have come from fruitful discussions with Nigel Wood and Alan Grant. I am also grateful to David Pick and Malcolm MacVean for swift and careful reviewing.

11 References

Beljaars,A.C.M. and Holtslag,A.A.M., 1991, Flux parametrization over Land Surfaces for Atmospheric Models., *J. Appl. Meteor.*, **30**, 327–341.

Blyth,E.M. and Culf,A.D, 1993, The effective roughness length for temperature in heterogeneous terrain: an example from the Sahelian Tiger Bush., *Annales Geophysicae*, Supplement II to Volume 11, Part II, European Geophysical Society.

Blyth,E.M., Dolman, A.J, and Wood,N., 1993, Effective resistance to sensible and latent heat flux in heterogeneous terrain. *Quart. J. Roy. Meteor. Soc.*, **119**, 423–442.

Brutsaert,W., 1975a, A theory for local evaporation (or heat transfer) from rough and smooth surfaces at ground level., *Water Res. Research*, **11**, 543-550.

Brutsaert,W., 1975b, The roughness length for water vapour, sensible heat, and other scalars. *J. Atmos. Sci.*, **32**, 2028–2031.

Brutsaert,W., 1979, Heat and mass transfer to and from surfaces with dense vegetation or similar permeable roughness. *Bound. Layer Meteor.*, **16**, 365–388.

Brutsaert,W., 1982, Evaporation into the Atmosphere. pp 299. D. Reidel Dordrecht.

Businger,J., 1988, A note on the Businger-Dyer profiles. *Bound. Layer Meteor.*, **42**, 145–151.

Chamberlain,A.C., 1966, Transport of gases to and from grass and grass-like surfaces. *Proc. R. Soc.*, **290**, 236-265.

Claussen,M., 1987, The flow in a turbulent boundary layer upstream of a change in surface roughness. *Bound. Layer Meteor.*, **40**, 31–86.

Claussen,M., 1990, Area-averaging of surface fluxes in a neutrally stratified, horizontally inhomogeneous atmospheric boundary layer., *Atmos. Environ.*, **24a**, 1349-1360.

Claussen,M., 1992, Scale aggregation in semi-smooth flow., Max-Planck-Institut for Meteorology Report No. 87, Hamburg.

De Bruin,H.A.R., Kohsiek,W. and Van Den Hurk,B.J.J.M., A verification of some methods to determine the fluxes of momentum, sensible heat and water vapour using standard deviation and structure parameter of scalar meteorological quantities. *Bound. Layer Meteor.*, **63**, 231–257.

Duynkerke,P.G., 1992, The Roughness Length for Heat and Other Vegetation Parameters for a Surface of Short Grass., *J. Appl. Meteor.*, **31**, 579–586.

Garratt,J.R., 1978, Transfer characteristics for a heterogeneous surface of large aerodynamic roughness., *Quart. J. Roy. Meteor. Soc.*, **104**, 491–502.

Garratt,J.R., 1992, The atmospheric boundary layer., pp 316, Cambridge atmospheric and space science series.

Garratt,J.R. and Hicks,B.B., 1973, Momentum, heat and water vapour transfer to and from natural and artificial surfaces., *Quart. J. Roy. Meteor. Soc.*, **99**, 680–687.

Grant,A.L.M. and Mason P.J., 1990, Observations of boundary layer structure over complex terrain., *Quart. J. Roy. Meteor. Soc.*, **116**, 159–186.

Hicks,B.B., 1981, An examination of turbulence statistics in the surface layer., *Bound. Layer Meteor.*, **21**, 389–402.

Hewer,F.E., 1992, The Effects of Orography on an Atmospheric General Circulation Model, MSc dissertation, Dept of Meteorology, University of Reading.

Kohsiek,W., De Bruin,H.A.R., The,H. and Van Den Hurk,B.J.J.M., Estimation of the sensible heat flux of a semi-arid area using surface radiative temperature measurements. *Bound. Layer Meteor.*, **63**, 213–230.

Kustas,W.P., Choudhury,B.J and Kunkel,K.E., 1989, A one- and two- layer model for estimating evapotranspiration with remotely sensed surface temperature and ground based meterorological data over partial canopy cover. 12th Canadian Symposium on Remote Sensing, Vancouver.

Lean, J., 1992, A Guide to the UK Meteorological Office Single Column Model., Bracknell, BERKS.

Lhomme,J-P, 1992, Energy balance of heterogeneous terrain: averaging the controlling parameters., *Agric. and Forest Met.*, **61**, 11-21.

Martin,R. and Maryon,R.H., 1992, A Description of the Air Mass Transformation Model. Met. O. (P) Special Investigations technical Memorandum No. 11.

Mason,P.J., 1988, The formation of areally averaged roughness lengths., *Quart. J. Roy. Meteor. Soc.*, **114**, 399–400.

Owen,P.R. and Thomson,W.R., 1963, Heat transfer across rough surfaces., *J. Fluid Mech.*, **15**, 321–334.

Panofsky,H.A., 1973, Tower Meteorology. Chapter 4 in Workshop on Micrometeorology, ed. D.A. Haugen, American Met. Soc.

Rider,N.E. and Robinson,G.D., 1951, A study of the transfer of heat and water vapour above a surface of short grass. *Quart. J. Roy. Meteor. Soc.*, **77**, 375–401.

Schmid,H.P. and Oke,T.R., 1990, A model to estimate the source area contributing to turbulent exchange in the surface layer over patchy terrain., *Quart. J. Roy. Meteor. Soc.*, **116**, 965–983.

Sheppard,P.A., 1958, Transfer across the Earth's surface through the air above. *Quart. J. Roy. Meteor. Soc.*, **84**, 205–224.

Shuttleworth,W.J., 1988, Macrohydrology - the new challenge for process hydrology., *J. Hydrol.*, **100**, 31-56.

Sugita,M. and Brutsaert,W., 1990, Regional surface fluxes from remotely sensed skin temperatures and lower boundary layer measurements., *Water Res. Research*, **26**, 2937-2944.

Verhoef,A and De Bruin, H.A.R., 1993, Determination and evaluation of a roughness length for heat., European Geophysical Society XVIII General Assembly, Wiesbaden.

Vihma,T. and Savijärvi,H., 1991, On the effective roughness length for heterogeneous terrain., *Quart. J. Roy. Meteor. Soc.*, **117**, 399–407.

Wieringa,J. 1976, An objective exposure correction method for averaging wind speeds measured at a sheltered location., *Quart. J. Roy. Meteor. Soc.*, **102**, 241–253.

Wieringa,J. 1986, Roughness-dependent geographical interpolation of surface wind speed averages,. *Quart. J. Roy. Meteor. Soc.*, **112**, 867–889.

Wood N. and Mason,P.J., 1991, The influence of static stability on the effective roughness lengths for momentum and heat transfer., *Quart. J. Roy. Meteor. Soc.*, **117**, 1025–1056.

12 Glossary.

B		Resistance ratio; sublayer Stanton number
C_D		Drag coefficient (u_*^2/U^2)
C_H		Transfer coefficient ($u_*T_*/U(T-T_s)$)
c_p	$Jkg^{-1}K^{-1}$	Specific heat capacity of air
d	m	Zero-plane displacement
E	$kgm^{-2}s^{-1}$	Evaporation rate from the surface
f_i		Fractional area of different surface types
g	ms^{-2}	Acceleration due to gravity (9.8 ms^{-2})
G	$W\,m^{-2}$	Ground heat flux
H	m	Boundary layer height
H_s	$W\,m^{-2}$	Sensible heat flux from the surface
k		von Kármán's constant (= 0.4)
$LAI(z)$		Leaf area index (ratio of total surface area of leaves / ground area below them)
L_m	m	Obukhov stability length ($u_*^3T_{ref}/kg\overline{w'T'}$)
$N[\mu,\sigma]$		Normal (Gaussian) distribution with mean μ and standard deviation σ
Pr		Prandtl number (≈ 0.7), ν/molecular diffusivity for heat ($\approx 2.1\times 10^{-5}m^2s^{-1}$)
R	$W\,m^{-2}$	Net radiation at the surface
Q	Kms^{-1}	Turbulent temperature flux
r_{am}	sm^{-1}	Momentum resistance ($1/C_DU$)
r_{ah}	sm^{-1}	Heat resistance ($1/C_DU$)
Re_*		Roughness Reynolds number (u_*z_{0m}/ν)
T	K	Temperature
T_s	K	Surface temperature
T_*	K	Reference temperature ($\overline{w'T'}/u_*$)
U	$m\,s^{-1}$	Wind speed
u'	$m\,s^{-1}$	Deviation from mean wind speed
$\overline{u'w'}$	$m^2\,s^{-2}$	Reynolds flux
u_*	$m\,s^{-1}$	Friction velocity

w	$m\ s^{-1}$	Vertical velocity
x	m	Horizontal coordinate
z	m	Height above the surface
z_{0m}	m	Roughness length for momentum
z_{0t}	m	Roughness length for temperature
α		Surface albedo
γ	K^{-1}	Psychrometric constant
ϵ_{sub}	sub	Standard error for quantity 'sub'
λ	Jkg^{-1}	Latent heat of vaporization for water
ν	m^2s^{-1}	Kinematic viscosity of air ($\approx 1.5 \times 10^{-5}$)
ρ	kgm^{-3}	Density
τ	Nm^{-2}	Surface stress
ϕ_H		Gradient profile function for heat. A universal function of z/L_m
ϕ_M		Gradient profile function for momentum. A universal function of z/L_m
ψ_H		Integral profile function for heat. Determined by integrating ϕ_H
ψ_M		Integral profile function for momentum. Determined by integrating ϕ_M